The Consultative Committee for Space Data Systems

Research and Development for
Space Data System Standards

LOW DENSITY PARITY CHECK CODES FOR USE IN NEAR-EARTH AND DEEP SPACE APPLICATIONS

EXPERIMENTAL SPECIFICATION

CCSDS 131.1-O-2

September 2007

The Consultative Committee for Space Data Systems

Research and Development for Space Data System Standards

LOW DENSITY PARITY CHECK CODES FOR USE IN NEAR-EARTH AND DEEP SPACE APPLICATIONS

EXPERIMENTAL SPECIFICATION

CCSDS 131.1-O-2

September 2007

AUTHORITY

Issue:	Orange Book, Issue 2
Date:	September 2007
Location:	Washington, DC, USA

This document has been approved for release by the Consultative Committee for Space Data Systems (CCSDS). The procedure for review and authorization of CCSDS documents is detailed in the *Procedures Manual for the Consultative Committee for Space Data Systems*.

This document is published and maintained by:

CCSDS Secretariat
Space Communications and Navigation Office, 7L70
Space Operations Mission Directorate
NASA Headquarters
Washington, DC 20546-0001, USA

FOREWORD

This document is a CCSDS Experimental specification for a set of Low Density Parity Check (LDPC) codes. It was contributed to CCSDS by NASA.

Through the process of normal evolution, it is expected that expansion, deletion, or modification of this document may occur. This Experimental Specification is therefore subject to CCSDS document management and change control procedures, which are defined in the *Procedures Manual for the Consultative Committee for Space Data Systems*. Current versions of CCSDS documents are maintained at the CCSDS Web site:

http://www.ccsds.org/

Questions relating to the contents or status of this document should be addressed to the CCSDS Secretariat at the address indicated on page i.

At time of publication, the active Member and Observer Agencies of the CCSDS were:

Member Agencies

- Agenzia Spaziale Italiana (ASI)/Italy.
- British National Space Centre (BNSC)/United Kingdom.
- Canadian Space Agency (CSA)/Canada.
- Centre National d'Etudes Spatiales (CNES)/France.
- Deutsches Zentrum für Luft- und Raumfahrt e.V. (DLR)/Germany.
- European Space Agency (ESA)/Europe.
- Federal Space Agency (FSA)/Russian Federation.
- Instituto Nacional de Pesquisas Espaciais (INPE)/Brazil.
- Japan Aerospace Exploration Agency (JAXA)/Japan.
- National Aeronautics and Space Administration (NASA)/USA.

Observer Agencies

- Austrian Space Agency (ASA)/Austria.
- Belgian Federal Science Policy Office (BFSPO)/Belgium.
- Central Research Institute of Machine Building (TsNIIMash)/Russian Federation.
- Centro Tecnico Aeroespacial (CTA)/Brazil.
- Chinese Academy of Sciences (CAS)/China.
- Chinese Academy of Space Technology (CAST)/China.
- Commonwealth Scientific and Industrial Research Organization (CSIRO)/Australia.
- Danish National Space Center (DNSC)/Denmark.
- European Organization for the Exploitation of Meteorological Satellites (EUMETSAT)/Europe.
- European Telecommunications Satellite Organization (EUTELSAT)/Europe.
- Hellenic National Space Committee (HNSC)/Greece.
- Indian Space Research Organization (ISRO)/India.
- Institute of Space Research (IKI)/Russian Federation.
- KFKI Research Institute for Particle & Nuclear Physics (KFKI)/Hungary.
- Korea Aerospace Research Institute (KARI)/Korea.
- MIKOMTEK: CSIR (CSIR)/Republic of South Africa.
- Ministry of Communications (MOC)/Israel.
- National Institute of Information and Communications Technology (NICT)/Japan.
- National Oceanic and Atmospheric Administration (NOAA)/USA.
- National Space Organization (NSPO)/Taiwan.
- Naval Center for Space Technology (NCST)/USA.
- Space and Upper Atmosphere Research Commission (SUPARCO)/Pakistan.
- Swedish Space Corporation (SSC)/Sweden.
- United States Geological Survey (USGS)/USA.

PREFACE

This document is a CCSDS Experimental Specification. Its Experimental status indicates that it is part of a research or development effort based on prospective requirements, and as such it is not considered a Standards Track document. Experimental Specifications are intended to demonstrate technical feasibility in anticipation of a 'hard' requirement that has not yet emerged. Experimental work may be rapidly transferred onto the Standards Track should a hard requirement emerge in the future.

DOCUMENT CONTROL

Document	Title	Date	Status
CCSDS 131.1-O-1	Low Density Parity Check Codes for Use in Near-Earth and Deep Space Applications, Experimental Specification, Issue 1	August 2006	Original issue, superseded
CCSDS 131.1-O-2	Low Density Parity Check Codes for Use in Near-Earth and Deep Space Applications, Experimental Specification, Issue 2	September 2007	Current issue: substantive changes from the original issue are indicated by change bars in the inside margin.
EC 1	Editorial Correction	October 2007	Corrects erroneous value in table A-1.
EC 2	Editorial Correction	June 2008	On page 2-7, last sentence, corrects reference to subsection of reference [1] from 6.6 to 6.3.

CONTENTS

CONTENTS (continued)

Figure Page

Table

1 INTRODUCTION

1.1 APPLICABILITY AND SCOPE

This CCSDS Experimental specification has been contributed to CCSDS by NASA. It describes a set of Low Density Parity Check (LDPC) codes including definition of their code structures, encoder implementations and experimental performance results.

This CCSDS Experimental specification is composed of two parts. The single rate 7/8 code described in section 2 was designed and optimized for the characteristics and requirements typical of many Near-Earth missions, whereas the set of codes described in section 3 was designed and optimized for the characteristics and requirements typical of many Deep-Space missions.

Users are cautioned that selection of the most appropriate code for a particular mission environment is a complex problem that involves evaluation of several characteristics, including:

- error rate performance, including error floors;
- encoder and decoder complexity, including the number of decoder iterations required to achieve desired performance;
- familial relationships between multiple codes;
- maturity and availability of implementations and implementation support;
- intellectual property issues;
- etc.

In addition, users may need to perform independent analysis and simulation. In order to begin the process of code selection, users are advised to approach the problem as follows:

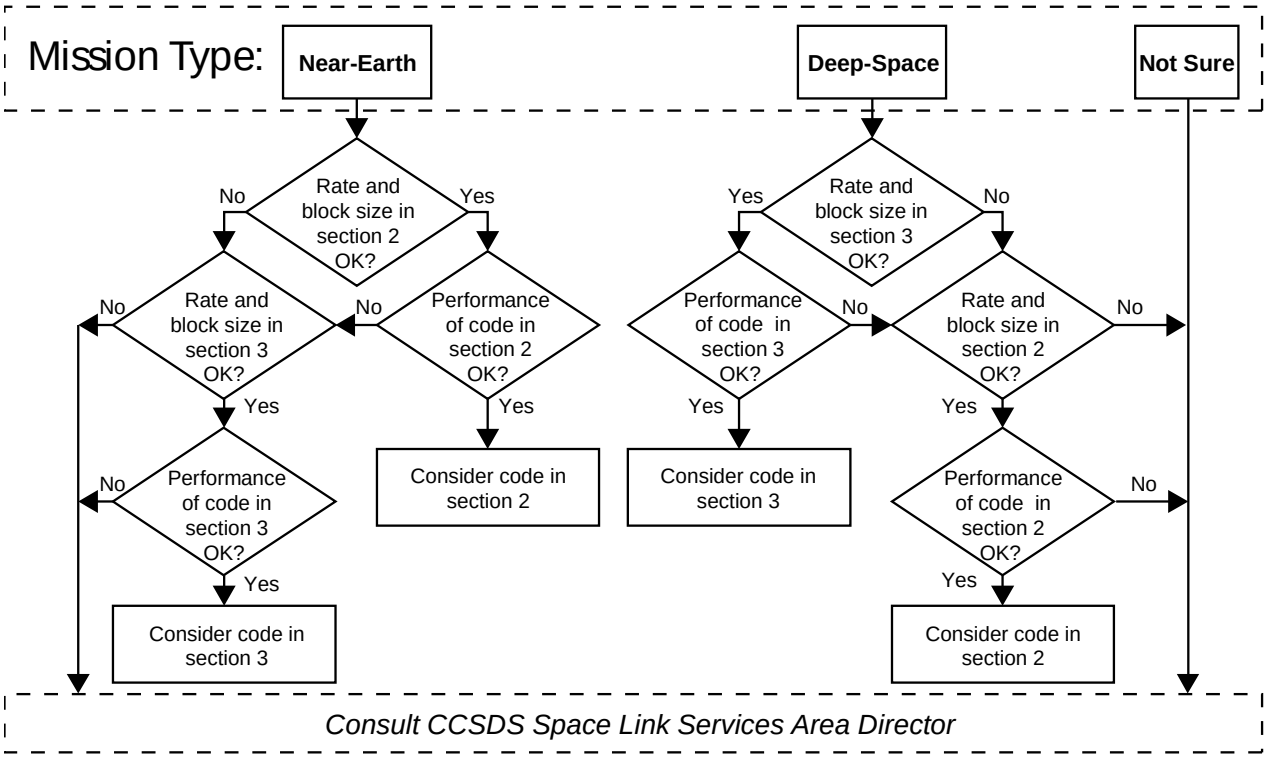

1.2 NOMENCLATURE

The following conventions apply throughout this Specification:

a) the words ‘shall’ and ‘must’ imply a binding and verifiable specification;

b) the word ‘should’ implies an optional, but desirable, specification;

c) the word ‘may’ implies an optional specification;

d) the words ‘is’, ‘are’, and ‘will’ imply statements of fact.

1.3 CONVENTIONS

In this document, the following convention is used to identify each bit in an *N*-bit field. The first bit in the field to be transmitted (i.e., the most left justified when drawing a figure) is defined to be ‘Bit 0’, the following bit is defined to be ‘Bit 1’, and so on up to ‘Bit *N*-1’. When the field is used to express a binary value (such as a counter), the Most Significant Bit (MSB) shall be the first transmitted bit of the field, i.e., ‘Bit 0’ (see figure 1-1).

Figure 1-1: Bit Numbering Convention

The convention for matrices differs from that for bit fields. Matrices are indexed beginning with the number ‘1’.

In accordance with standard data-communications practice, data fields are often grouped into 8-bit ‘words’ which conform to the above convention. Throughout this Specification, such an 8-bit word is called an ‘octet’.

The numbering for octets within a data structure starts with ‘0’.

1.4 REFERENCES

The following document contains provisions which, through reference in this text, constitute provisions of this Experimental Specification. At the time of publication, the edition indicated was valid. All documents are subject to revision, and users of this Experimental Specification are encouraged to investigate the possibility of applying the most recent edition of the document indicated below. The CCSDS Secretariat maintains a register of currently valid CCSDS documents.

[1] *TM Synchronization and Channel Coding*. Recommendation for Space Data System Standards, CCSDS 131.0-B-1. Blue Book. Issue 1. Washington, D.C.: CCSDS, September 2003.

NOTE – Annex C contains lists of informative references.

2 LOW DENSITY PARITY CHECK CODE OPTIMIZED FOR NEAR EARTH APPLICATIONS

2.1 OVERVIEW

2.1.1 BACKGROUND

The mid-1990s were highlighted by the rediscovery of Low Density Parity Check codes (LDPCC) in the field of channel coding (reference [C1.1]). Originally invented by R. Gallager in his PhD thesis in 1961 (reference [C1.2]), this coding technique was largely forgotten for more than 30 years. The primary advance in LDPCC is the discovery of an iterative decoding algorithm, now called Belief Propagation (BP) decoding, which offers near-optimum performance for large linear LDPCC at a manageable complexity. LDPCC performance gains were difficult to realize technologically in the early 1960s. Several decades of VLSI development has finally made the implementation of these codes practical.

The original construction, now called Gallager LDPCC, has come to be regarded as a special class of LDPCC. Recent advances in LDPC code construction have resulted in the development of new codes with (arguably) improved performance over Gallager LDPCC. One class of these codes, irregular LDPCC (reference [C1.3]), demonstrates improved performance in the waterfall region. Disadvantages of irregular codes, however, include an increase, in general, in the number of iterations required for decoding convergence and an unequal error protection between code bits resulting from the irregular structure. Another class of LDPCC developed using algebraic construction based on finite geometries (reference [C1.4]) has been shown to provide very low error floors and very fast iterative convergence. These qualities make these codes a good fit for near Earth applications where very high data rates and high reliability are the driving requirements. A white paper based on Euclidean Geometry LDPCC (reference [C1.5]) was submitted to the CCSDS Channel Coding Subpanel P1B in the fall 2002 Houston meeting. That paper and subsequent research is the basis for the code presented in this Experimental Specification.

2.1.2 TECHNICAL FOUNDATION

A linear block code is designated in this Experimental Specification by (n, k) where n is the length of the codeword (or block) and k is the length of the information sequence. LDPC codes are linear block codes in which the ratio of the total number of '1's to the total number of elements in the parity check matrix is << 0.5. The distribution of the '1's determine the structure and performance of the decoder. An LDPC code is defined by its parity check matrix. The $k \times n$ generator matrix which is used to encode a linear block code can be derived from the parity check matrix through linear operations. (The reader is encouraged to review reference [C1.8] for an overview of linear block codes).

The LDPC code considered in this specification is a member of a class of codes called Quasi-Cyclic codes. The construction of these codes involves juxtaposing smaller circulants (or cyclic submatrices) to form a larger parity check or base matrix.

An example of a circulant is shown in figure 2-1. Notice that every row is one bit right cyclic shift (where the end bit is wrapped around to the beginning bit) of the previous row. The entire circulant is uniquely determined and specified by its first row. For this example the first row has four '1's or a row weight of four.

$$\begin{bmatrix}
0&0&0&0&0&0&0&1&1&0&1&0&0&0&1\\
1&0&0&0&0&0&0&0&1&1&0&1&0&0&0\\
0&1&0&0&0&0&0&0&0&1&1&0&1&0&0\\
0&0&1&0&0&0&0&0&0&0&1&1&0&1&0\\
0&0&0&1&0&0&0&0&0&0&0&1&1&0&1\\
1&0&0&0&1&0&0&0&0&0&0&0&1&1&0\\
0&1&0&0&0&1&0&0&0&0&0&0&0&1&1\\
1&0&1&0&0&0&1&0&0&0&0&0&0&0&1\\
1&1&0&1&0&0&0&1&0&0&0&0&0&0&0\\
0&1&1&0&1&0&0&0&1&0&0&0&0&0&0\\
0&0&1&1&0&1&0&0&0&1&0&0&0&0&0\\
0&0&0&1&1&0&1&0&0&0&1&0&0&0&0\\
0&0&0&0&1&1&0&1&0&0&0&1&0&0&0\\
0&0&0&0&0&1&1&0&1&0&0&0&1&0&0\\
0&0&0&0&0&0&1&1&0&1&0&0&0&1&0
\end{bmatrix}$$

Figure 2-1: Example of a 15 × 15 Circulant Matrix

An example of a quasi-cyclic parity check matrix is shown in figure 2-2. In this case, a quasi-cyclic 10 × 25 matrix is formed by an array of 2 × 5 circulant submatrices of size 5 × 5. To unambiguously describe this matrix, only the position of the '1's in the first row of every circulant submatrix and the location of each submatrix within the base matrix is needed.

$$\begin{bmatrix}
1&0&0&1&0&1&1&0&0&0&0&1&0&0&1&0&1&1&0&0&1&0&0&0&1\\
0&1&0&0&1&0&1&1&0&0&1&0&1&0&0&0&0&1&1&0&1&1&0&0&0\\
1&0&1&0&0&0&0&1&1&0&0&1&0&1&0&0&0&0&1&1&0&1&1&0&0\\
0&1&0&1&0&0&0&0&1&1&0&0&1&0&1&1&0&0&0&1&0&0&1&1&0\\
0&0&1&0&1&1&0&0&0&1&1&0&0&1&0&1&1&0&0&0&0&0&0&1&1\\
0&1&0&0&1&0&0&0&1&1&0&0&1&0&1&1&0&1&0&0&1&1&0&0&0\\
1&0&1&0&0&1&0&0&0&1&1&0&0&1&0&0&1&0&1&0&0&1&1&0&0\\
0&1&0&1&0&1&1&0&0&0&0&1&0&0&1&0&0&1&0&1&0&0&1&1&0\\
0&0&1&0&1&0&1&1&0&0&1&0&1&0&0&1&0&0&1&0&0&0&0&1&1\\
1&0&0&1&0&0&0&1&1&0&0&1&0&1&0&0&1&0&0&1&1&0&0&0&1
\end{bmatrix}$$

Figure 2-2: Example of a Quasi-Cyclic Matrix

Constructing parity check matrices in this manner produces two positive features:

a) the encoding complexity can be made linear with the code length or parity bits using shift registers, and

b) encoder and decoder routing complexity in the interconnections of integrated circuits is reduced.

2.2 BASE (8176,7156) LDPC CODE

This section describes the base (8176, 7156) LDPC code. For reasons outlined below, implementations should shorten the base code according to the format described in subsection 2.5. The parity check matrix for the (8176, 7156) LDPC code is formed by using a 2 × 16 array of 511 × 511 square circulants. This creates a parity check matrix of dimension 1022 × 8176. The structure of the parity check base matrix is shown in figure 2-3.

$$\begin{bmatrix} A_{1,1} & A_{1,2} & A_{1,3} & A_{1,4} & A_{1,5} & A_{1,6} & A_{1,7} & A_{1,8} & A_{1,9} & A_{1,10} & A_{1,11} & A_{1,12} & A_{1,13} & A_{1,14} & A_{1,15} & A_{1,16} \\ A_{2,1} & A_{2,2} & A_{2,3} & A_{2,4} & A_{2,5} & A_{2,6} & A_{2,7} & A_{2,8} & A_{2,9} & A_{2,10} & A_{2,11} & A_{2,12} & A_{2,13} & A_{2,14} & A_{2,15} & A_{2,16} \end{bmatrix}$$

Figure 2-3: Base Parity Check Matrix of the (8176, 7156) LDPC Code

Each $A_{i,j}$ is a 511 × 511 circulant. The row weight of the each of the 32 circulants is two; i.e., there are two '1's in each row. The total row weight of each row in the parity check matrix is 2 × 16, or 32. The column weight of each circulant is also two; i.e., there are two '1's in each column. The total weight of each column in the parity check matrix is 2 × 2 or four. The position of the '1's in each circulant is defined in table 2-1. A scatter chart of the parity check matrix is shown in figure 2-4 where every '1' bit in the matrix is represented by a point.

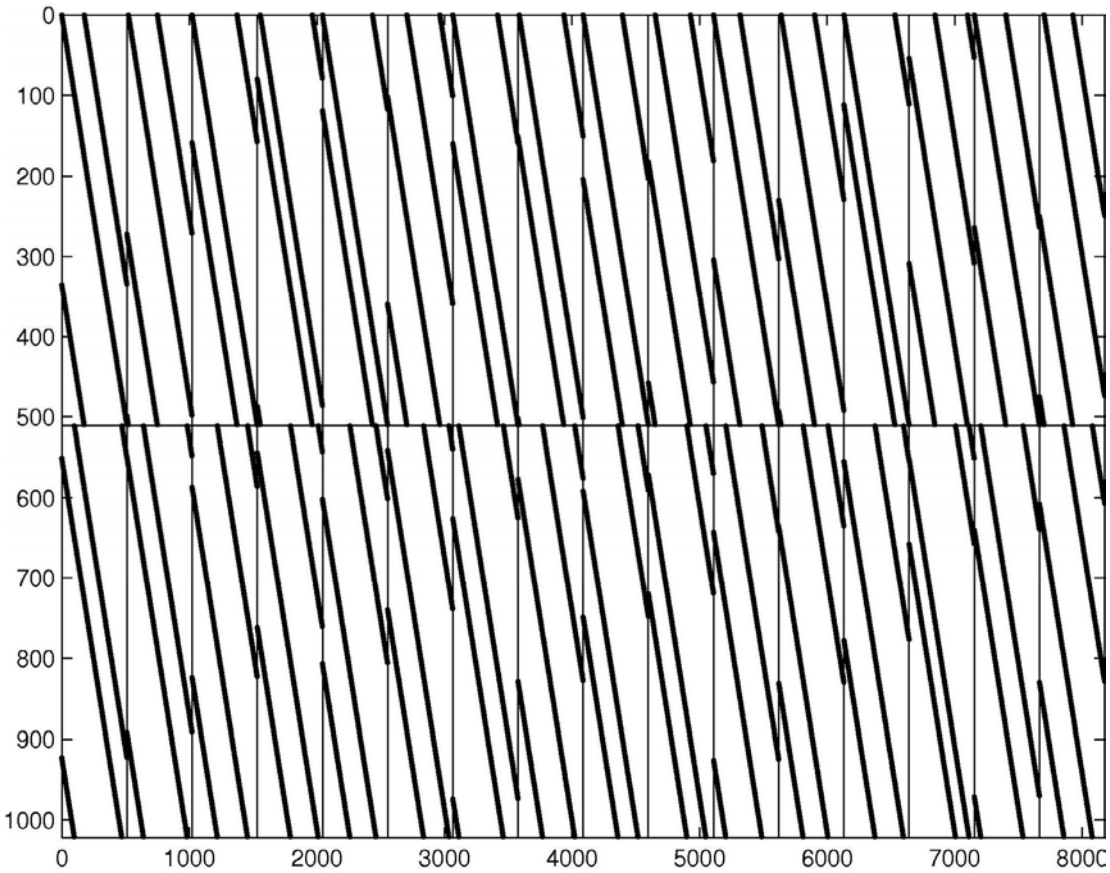

Figure 2-4: Scatter Chart of Parity Check Matrix

Table 2-1: Specification of Circulants

Circulant	'1's position in 1st row of circulant	Absolute '1's position in 1st row of Parity Check Matrix
$A_{1,1}$	0, 176	0, 176
$A_{1,2}$	12, 239	523, 750
$A_{1,3}$	0, 352	1022, 1374
$A_{1,4}$	24, 431	1557, 1964
$A_{1,5}$	0, 392	2044, 2436
$A_{1,6}$	151, 409	2706, 2964
$A_{1,7}$	0, 351	3066, 3417
$A_{1,8}$	9, 359	3586, 3936
$A_{1,9}$	0, 307	4088, 4395
$A_{1,10}$	53, 329	4652, 4928
$A_{1,11}$	0, 207	5110, 5317
$A_{1,12}$	18, 281	5639, 5902
$A_{1,13}$	0, 399	6132, 6531
$A_{1,14}$	202, 457	6845, 7100
$A_{1,15}$	0, 247	7154, 7401
$A_{1,16}$	36, 261	7701, 7926
$A_{2,1}$	99, 471	99, 471
$A_{2,2}$	130, 473	641, 984
$A_{2,3}$	198, 435	1220, 1457
$A_{2,4}$	260, 478	1793, 2011
$A_{2,5}$	215, 420	2259, 2464
$A_{2,6}$	282, 481	2837, 3036
$A_{2,7}$	48, 396	3114, 3462
$A_{2,8}$	193, 445	3770, 4022
$A_{2,9}$	273, 430	4361, 4518
$A_{2,10}$	302, 451	4901, 5050
$A_{2,11}$	96, 379	5206, 5489
$A_{2,12}$	191, 386	5812, 6007
$A_{2,13}$	244, 467	6376, 6599
$A_{2,14}$	364, 470	7007, 7113
$A_{2,15}$	51, 382	7205, 7536
$A_{2,16}$	192, 414	7857, 8079

Note that the numbers in the second column represent the relative column position of the '1's in the first row of each circulant. Since there are only 511 possible positions, these numbers can range only from 0 to 510. The third column represents the absolute position of the '1's in the parity check matrix. There are exactly 8176 possible; therefore these numbers can range only from 0 to 8175.

2.3 ENCODING

The encoder can be designed using the method given in reference [C1.6]. The generator matrix of the (8176, 7156) code consists of two parts. The first part is a 7154 × 8176 submatrix in systematic-circulant form as shown in figure 2-5. It consists of a 7154 × 7154 identity matrix and two columns of 511 × 511 circulants $B_{i,j}$s, each column consisting of 14 circulants. The Is are the 511 × 511 identity submatrices and the 0s are the all zero 511 × 511 submatrices. The second part consists of two independent rows. The first part generates a (8176, 7154) LDPC subcode of the (8176, 7156) code. Each codeword in the subcode consists of 7154 information bits and 1022 parity check bits. For reason given in section 2.4, there are advantages in using the subcode implementation. The circulants $B_{i,j}$s are constructed based on the algorithm given below:

1) From figure 2-3 and table 2-1, define $\mathrm{D} = \begin{bmatrix} \mathrm{A}_{1,15} & \mathrm{A}_{1,16} \\ \mathrm{A}_{2,15} & \mathrm{A}_{2,16} \end{bmatrix}$, which is a 1022×1022 matrix.

2) Let u = (1 0 0 0 …. 0) be the unit 511 tuple, i.e., a vector quantity of length 511 with a '1' at the leftmost position and '0's in the rest.

3) Define $z_i = (b_{i,1} \quad b_{i,2})$, where i = 1, 2, ..., 14 and the $b_{i,j}$s are the first row of the $B_{i,j}$ circulants.

4) Define $\mathrm{M}_i = \begin{bmatrix} \mathrm{A}_{1,i} \\ \mathrm{A}_{2,i} \end{bmatrix}$, where i = 1, 2, …, 14. (Note that the parity check matrix can now be represented as: $[\mathrm{M}_1\ \mathrm{M}_2 \ldots \mathrm{M}_{14}\ \mathrm{D}]$.)

5) Since the rank of D is 1020 and not 1022, there are two linearly dependent columns, 511th and 1022nd. Set the 511th and 1022nd elements of z_i to zero and solve $\mathrm{M}_i u^{\mathrm{T}} + \mathrm{D} z_i^{\mathrm{T}} = 0$ for z_i, where i = 1, 2, …, 14 and T superscript represents matrix transpose.

6) The $b_{i,j}$s can be extracted from the z_is. (They are numerically tabulated in annex A1.)

There are many ways to design the encoder based on the generator matrix in figure 2-5. These schemes have complexities that are proportional to the length of the codeword or parity check bits (see reference [C1.6]).

$$\begin{bmatrix}
I & 0 & 0 & 0 & 0 & 0 & 0 & 0 & 0 & 0 & 0 & 0 & 0 & 0 & B_{1,1} & B_{1,2} \\
0 & I & 0 & 0 & 0 & 0 & 0 & 0 & 0 & 0 & 0 & 0 & 0 & 0 & B_{2,1} & B_{2,2} \\
0 & 0 & I & 0 & 0 & 0 & 0 & 0 & 0 & 0 & 0 & 0 & 0 & 0 & B_{3,1} & B_{3,2} \\
0 & 0 & 0 & I & 0 & 0 & 0 & 0 & 0 & 0 & 0 & 0 & 0 & 0 & B_{4,1} & B_{4,2} \\
0 & 0 & 0 & 0 & I & 0 & 0 & 0 & 0 & 0 & 0 & 0 & 0 & 0 & B_{5,1} & B_{5,2} \\
0 & 0 & 0 & 0 & 0 & I & 0 & 0 & 0 & 0 & 0 & 0 & 0 & 0 & B_{6,1} & B_{6,2} \\
0 & 0 & 0 & 0 & 0 & 0 & I & 0 & 0 & 0 & 0 & 0 & 0 & 0 & B_{7,1} & B_{7,2} \\
0 & 0 & 0 & 0 & 0 & 0 & 0 & I & 0 & 0 & 0 & 0 & 0 & 0 & B_{8,1} & B_{8,2} \\
0 & 0 & 0 & 0 & 0 & 0 & 0 & 0 & I & 0 & 0 & 0 & 0 & 0 & B_{9,1} & B_{9,2} \\
0 & 0 & 0 & 0 & 0 & 0 & 0 & 0 & 0 & I & 0 & 0 & 0 & 0 & B_{10,1} & B_{10,2} \\
0 & 0 & 0 & 0 & 0 & 0 & 0 & 0 & 0 & 0 & I & 0 & 0 & 0 & B_{11,1} & B_{11,2} \\
0 & 0 & 0 & 0 & 0 & 0 & 0 & 0 & 0 & 0 & 0 & I & 0 & 0 & B_{12,1} & B_{12,2} \\
0 & 0 & 0 & 0 & 0 & 0 & 0 & 0 & 0 & 0 & 0 & 0 & I & 0 & B_{13,1} & B_{13,2} \\
0 & 0 & 0 & 0 & 0 & 0 & 0 & 0 & 0 & 0 & 0 & 0 & 0 & I & B_{14,1} & B_{14,2}
\end{bmatrix}$$

Figure 2-5: Systematic Circulant Generator Matrix

2.4 SHORTENED (8160, 7136) CODE

Using the generator matrix given by figure 2-5, an encoder can be implemented using a circuit described in reference [C1.6]. This encoder generates a (8176, 7154) LDPC subcode of the (8176, 7156) code. Current spacecraft and ground systems manipulate and process data at 32-bit computer word size. Neither (8176, 7154) nor (8176, 7156) is a multiple of 32. It is beneficial to shorten the codeword to the dimensions of (8160, 7136). In other words, by shortening the information sequence to 7136 through the use of 18 bits of virtual fill, the (8176, 7154) subcode encoder can be used. This is accomplished by encoding the virtual fill bits with zeros but not transmitting them; thus the total codeword length becomes 8158. Note that it is not necessary to add two independent rows to the generator matrix to encode the full (8176, 7156) code because these bits would be shortened anyway, and so the subcode is sufficient and less complicated for this application. Since the code length of 8158 is two bits shy of 8160, an exact multiple of 32, two bits of actual transmitted zero fill are appended to the end of the codeword to achieve a shortened code dimension of (8160, 7136) bits, or (1020, 892) octets, or (255, 223) 32-bit words. The shortened codeword is shown in figure 2-6.

The received shortened codeword would require the removal of the two zero fill bits prior to decoding. The decoder would then reproduce the 18 virtual fill zeros after processing but would, in general, not pass these 18 zeros on to the ground equipment.

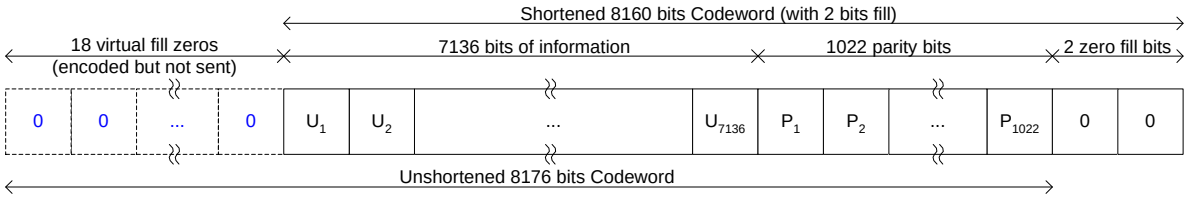

Figure 2-6: Shortened Codeword

2.5 RANDOMIZATION AND SYNCHRONIZATION

The use of the shortened (8160, 7136) LDPC code does not guarantee sufficient bit (symbol) transitions to acquire or maintain bit (symbol) synchronization. It is highly recommended that a pseudo-randomizer be used after encoding in accordance with section 7 of reference [1].

In addition, frame (codeword) synchronization is required so that the receiver can identify the beginning of the frame (codeword) for proper decoding. The use of an attached sync marker (ASM) as specified in subsection 6.3 of reference [1] is required. Note that the ASM is not pseudo-randomized.

3 LOW DENSITY PARITY CHECK CODE FAMILY OPTIMIZED FOR DEEP SPACE APPLICATIONS

3.1 OVERVIEW

3.1.1 BACKGROUND

The Low-Density Parity-Check (LDPC) codes presented in this document are intended to complement the current codes in the CCSDS Recommended Standard, *TM Synchronization and Channel Coding* (reference [1]), and were designed according to a list of requirements and evaluation criteria that reflect the needs of spacecraft applications (see references [C2.1] and [C2.2]).

– Requirements

  • *Code rates*: The family shall include codes of rate ≈ 0.5 and ≈ 0.8

  • *Block lengths*: The family shall cover k≈1000 to k≈16000 information bits spaced by multiples of ≈ 4

  • *Family*: A single hardware decoder shall be appropriate for all codes

  • *Intellectual property*: There must be no restrictions for CCSDS members

– Desired Properties

  • *Systematic encoders*: Systematic encoders are preferred

  • *Code rates*: One or two intermediate rates from {1/2,2/3,3/4,4/5} are desired

– Evaluation Criteria

  • *Decoder computation*: Codes requiring fewer decoder message computations are preferred

  • *Encoder computation*: Preferred encoders require fewer logic gates for a given speed

  • *Description complexity*: The code description in a standards document should be short

  • *Code performance*: Codes requiring less E_b/N_0 at Word Error Rate (WER)=10^{-4} and 10^{-6} are preferred

The selected code rates are 1/2, 2/3, and 4/5, three values, which are about uniformly spaced by 1 dB on the rate-dependent capacity curve for the binary-input Additive White Gaussian Noise (AWGN) channel (reference [C2.6]). Near rate 1/2, a 1% improvement in bandwidth efficiency costs about 0.02 dB in power efficiency; near rate 7/8, a 1% improvement in bandwidth efficiency costs 0.1 dB in power efficiency. Hence, the use of a higher order modulation may be a more practical means for saving bandwidth than the use of a code with

rate much above 0.8. The code rates are exact ratios of small integers to simplify implementation.

The selected block lengths are k=1024, k=4096, and k=16384. The three values k={1024,4096,∞} are about uniformly spaced by 0.6 dB on the sphere-packing bound at WER=10^{-8}, and reducing the last value from ∞ to 16384 makes the largest block size practical at a cost of about 0.3 dB. By choosing to keep k constant among family members, rather than n, the spacecraft's command and data handling system can generate data frames without knowledge of the code rate. Choosing powers of 2 may simplify implementation.

Implementers should be aware that many patents have been filed on LDPC codes; in particular, a procedure for parallelized decoding of LDPC codes is covered by a U.S. patent granted to T. Richardson and V. Novichkov.[1]

The selected codes are systematic. A low-complexity encoding method is described (see reference [C2.5]). The parity check matrices have plenty of structure to facilitate decoder implementation (see reference [C2.8]). The codes have irregular degree distributions, because this improves performance by about 0.5 dB at rate 1/2, compared to a regular (3,6) code (see reference [C2.3]). Naming conventions proposed in references [C2.1] and [C2.2] have designated these codes Accumulate-Repeat-4-Jagged-Accumulate (AR4JA).

3.1.2 DESCRIPTION OF THE CODE

Like turbo codes, low-density parity-check (LDPC) codes are binary block codes with large code blocks (hundreds or thousands of bits). They may be systematic or non-systematic, and they may be transparent or non-transparent. The nine LDPC codes defined here are systematic. All are non-transparent,[2] and phase ambiguities are resolved using frame markers, which are required for Codeblock synchronization.

Like turbo codes, LDPC codes may be used to obtain greater coding gain than those provided by concatenated coding systems. In contrast to turbo codes, LDPC codes offer the prospect of much higher decoding speeds via highly parallelized decoder structures. Currently reference [1] includes turbo codes of rates 1/2 and lower and a convolutional code of rate 1/2. LDPC codes of rates 1/2 and higher are defined in this experimental specification. Therefore rate 1/2 is the only rate at which this specification and reference [1] are comparable.

[1] Richardson, Tom, and Novichkov, Vladimir. 2001. Methods and apparatus for decoding LDPC codes. U.S. Patent 6,633,856, filed October 10, 2001, and issued October 14, 2003.

[2] Differential encoding (i.e., NRZ-M signaling) after the LDPC encoder is not recommended since soft decoding would require the use of differential detection with considerable loss of performance. Differential encoding before the LDPC encoder cannot be used because the LDPC codes specified in this document are non-transparent. This implies that phase ambiguities have to be detected and resolved by the frame synchronizer.

NOTES

1 LDPC coding, by itself, cannot guarantee sufficient bit transitions to keep receiver symbol synchronizers in lock. Therefore, the Pseudo-Randomizer defined in reference [1] is required unless the system designer verifies that sufficient symbol transition density is assured by other means when the Randomizer is not used.

2 The AR4JA LDPC codes proposed in this document posses relatively large minimum distance for their block length and undetected error rates lie several orders of magnitude below detected frame and bit error rates for any given operating signal-to-noise ratio. In many applications, therefore, frame validation can be achieved by simply checking the parity of an estimated codeword. In cases where the undetected frame error rate must be guaranteed to lie below a given threshold, then the designer may opt to append parity from a cyclic redundancy code with known distance.

3.2 SPECIFICATION

An LDPC code is specified indirectly by a v-by-w parity-check matrix H consisting of v linearly independent rows. A coded sequence of w bits must satisfy all v parity-check equations corresponding to the v rows of H. Parity-check matrices may include additional linearly dependent rows without changing the code. An encoder maps an input frame of $k \leq w-v$ information bits uniquely into a codeblock of $n \leq w$ bits. If $n<w$, the remaining $w-n$ code symbols are punctured and are not transmitted. If $k<w-v$, the remaining dimensions of the code remain unused.

The codeblock lengths n and information block lengths k, and the corresponding rates $r=k/n$, are shown in table 3-1 for the suite of LDPC codes. The LDPC code rates r are exactly as indicated in table 3-1, unlike the case of turbo codes for which the precise code rates are slightly lower than the corresponding nominal rates due to termination bits.

Table 3-1: Codeblock Lengths for Supported Code Rates (Measured in Bits)

Information block length k	Code block length n		
	rate 1/2	rate 2/3	rate 4/5
1024	2048	1536	1280
4096	8192	6144	5120
16384	32768	24576	20480

Table 3-2: Values of Submatrix Size *M* for Supported Codes

Information block length k	Submatrix size M		
	rate 1/2	rate 2/3	rate 4/5
1024	512	256	128
4096	2048	1024	512
16384	8192	4096	2048

For each (n, k) in table 3-1, a parity-check matrix H is defined below.

3.3 PARITY CHECK MATRICES

The *H* matrices are constructed from *M*×*M* submatrices, where the submatrix size is listed in table 3-2.

The *H* matrices for the rate-1/2 codes are specified as follows,

$$H_{1/2} = \begin{bmatrix} 0_M & 0_M & I_M & 0_M & I_M \oplus \Pi_1 \\ I_M & I_M & 0_M & I_M & \Pi_2 \oplus \Pi_3 \oplus \Pi_4 \\ I_M & \Pi_5 \oplus \Pi_6 & 0_M & \Pi_7 \oplus \Pi_8 & I_M \end{bmatrix}$$

where I_M and 0_M are the *M*×*M* identity and zero matrices, respectively, and Π_1 through Π_8 are permutation matrices. The *H* matrices for the rate-2/3 and rate-4/5 codes are specified with additional columns and permutation matrices as follows. An *H* matrix for rate-3/4 is also specified since this rate naturally occurs via the column extension required to achieve rate-4/5.

$$H_{2/3} = \left[\begin{array}{cc|c} 0_M & 0_M & \\ \Pi_9 \oplus \Pi_{10} \oplus \Pi_{11} & I_M & H_{1/2} \\ I_M & \Pi_{12} \oplus \Pi_{13} \oplus \Pi_{14} & \end{array}\right]$$

$$H_{3/4} = \left[\begin{array}{cc|c} 0_M & 0_M & \\ \Pi_{15} \oplus \Pi_{16} \oplus \Pi_{17} & I_M & H_{2/3} \\ I_M & \Pi_{18} \oplus \Pi_{19} \oplus \Pi_{20} & \end{array}\right]$$

$$H_{4/5} = \left[\begin{array}{cc|c} 0_M & 0_M & \\ \Pi_{21} \oplus \Pi_{22} \oplus \Pi_{23} & I_M & H_{3/4} \\ I_M & \Pi_{24} \oplus \Pi_{25} \oplus \Pi_{26} & \end{array}\right]$$

Permutation matrix Π_k has non-zero entries in row i and column $\pi_k(i)$ for $i \in \{0,..., M\text{-}1\}$ and

$$\pi_k(i) = \frac{M}{4}\left(\left(\theta_k + \lfloor 4i/M \rfloor\right) \bmod 4\right) + \left(\phi_k\left(\lfloor 4i/M \rfloor, M\right) + i\right) \bmod \frac{M}{4}$$

where the functions θ_k and $\phi_k(j, M)$ are defined in table 3-3 and table 3-4. Values defined in these tables describe $\phi_k(j, M)$'s using 7-tuples where consecutive positions in a tuple correspond to submatrix sizes from the set *M*={128, 256, 512, 1024, 2048, 4096, 8192}. The parity check matrix descriptions in conjunction with table 3-3 and table 3-4 describe 28

codes, one for each rate r = {1/2, 2/3, 3/4, 4/5} and M in the set above. Of these 28 codes, 9 are selected based on criteria provided earlier in this document (for instance spacing of ~1dB for different rates and 0.6 dB for different lengths). For any of the H matrices constructed per this description the last M code symbols are to be punctured (not transmitted). For example, the parity matrix for the (n = 1280, k = 1024) rate-4/5 code is shown below with blue lines representing each non-zero circulant entry, and structure indicated by gridlines. Minor gridlines are spaced at intervals m and major gridlines (not shown) at $M = 4m$.

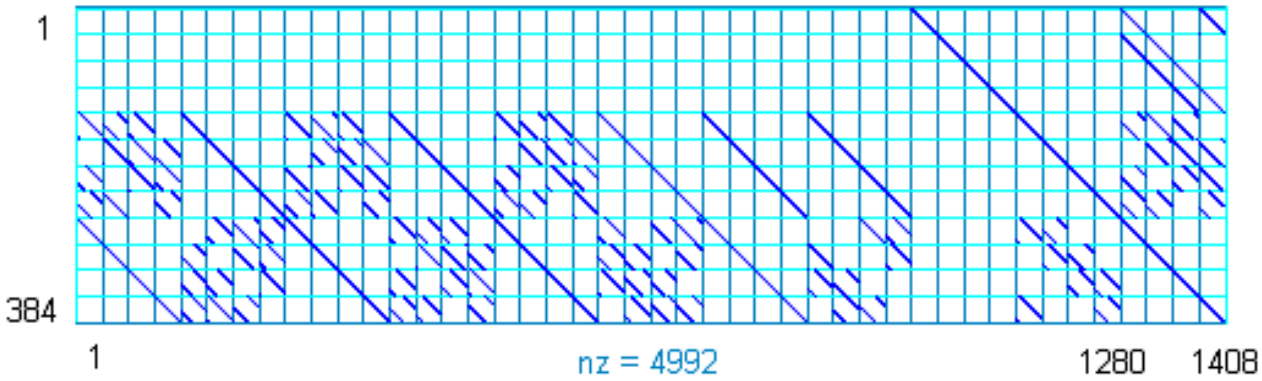

Figure 3-1: An *H* Matrix for the (*n* = 1280, *k* = 1024) Rate 4/5 Code

NOTE – For this code M=128 and columns 1281 through 1408 are punctured.

Table 3-3: Description of $\phi_k(0,M)$ and $\phi_k(1,M)$

k	θ_k	$\phi_k(0,M)$ $M = 2^7 \ldots 2^{13}$							$\phi_k(1,M)$ $M = 2^7 \ldots 2^{13}$						
1	3	1	59	16	160	108	226	1148	0	0	0	0	0	0	0
2	0	22	18	103	241	126	618	2032	27	32	53	182	375	767	1822
3	1	0	52	105	185	238	404	249	30	21	74	249	436	227	203
4	2	26	23	0	251	481	32	1807	28	36	45	65	350	247	882
5	2	0	11	50	209	96	912	485	7	30	47	70	260	284	1989
6	3	10	7	29	103	28	950	1044	1	29	0	141	84	370	957
7	0	5	22	115	90	59	534	717	8	44	59	237	318	482	1705
8	1	18	25	30	184	225	63	873	20	29	102	77	382	273	1083
9	0	3	27	92	248	323	971	364	26	39	25	55	169	886	1072
10	1	22	30	78	12	28	304	1926	24	14	3	12	213	634	354
11	2	3	43	70	111	386	409	1241	4	22	88	227	67	762	1942
12	0	8	14	66	66	305	708	1769	12	15	65	42	313	184	446
13	2	25	46	39	173	34	719	532	23	48	62	52	242	696	1456
14	3	25	62	84	42	510	176	768	15	55	68	243	188	413	1940
15	0	2	44	79	157	147	743	1138	15	39	91	179	1	854	1660
16	1	27	12	70	174	199	759	965	22	11	70	250	306	544	1661
17	2	7	38	29	104	347	674	141	31	1	115	247	397	864	587
18	0	7	47	32	144	391	958	1527	3	50	31	164	80	82	708
19	1	15	1	45	43	165	984	505	29	40	121	17	33	1009	1466
20	2	10	52	113	181	414	11	1312	21	62	45	31	7	437	433
21	0	4	61	86	250	97	413	1840	2	27	56	149	447	36	1345
22	1	19	10	1	202	158	925	709	5	38	54	105	336	562	867
23	2	7	55	42	68	86	687	1427	11	40	108	183	424	816	1551
24	1	9	7	118	177	168	752	989	26	15	14	153	134	452	2041
25	2	26	12	33	170	506	867	1925	9	11	30	177	152	290	1383
26	3	17	2	126	89	489	323	270	17	18	116	19	492	778	1790

Table 3-4: Description of $\phi_k(2,M)$ and $\phi_k(3,M)$

		$\phi_k(2,M)$							$\phi_k(3,M)$						
		$M = 2^7 \ldots 2^{13}$							$M = 2^7 \ldots 2^{13}$						
k	θ_k														
1	3	0	0	0	0	0	0	0	0	0	0	0	0	0	0
2	0	12	46	8	35	219	254	318	13	44	35	162	312	285	1189
3	1	30	45	119	167	16	790	494	19	51	97	7	503	554	458
4	2	18	27	89	214	263	642	1467	14	12	112	31	388	809	460
5	2	10	48	31	84	415	248	757	15	15	64	164	48	185	1039
6	3	16	37	122	206	403	899	1085	20	12	93	11	7	49	1000
7	0	13	41	1	122	184	328	1630	17	4	99	237	185	101	1265
8	1	9	13	69	67	279	518	64	4	7	94	125	328	82	1223
9	0	7	9	92	147	198	477	689	4	2	103	133	254	898	874
10	1	15	49	47	54	307	404	1300	11	30	91	99	202	627	1292
11	2	16	36	11	23	432	698	148	17	53	3	105	285	154	1491
12	0	18	10	31	93	240	160	777	20	23	6	17	11	65	631
13	2	4	11	19	20	454	497	1431	8	29	39	97	168	81	464
14	3	23	18	66	197	294	100	659	22	37	113	91	127	823	461
15	0	5	54	49	46	479	518	352	19	42	92	211	8	50	844
16	1	3	40	81	162	289	92	1177	15	48	119	128	437	413	392
17	2	29	27	96	101	373	464	836	5	4	74	82	475	462	922
18	0	11	35	38	76	104	592	1572	21	10	73	115	85	175	256
19	1	4	25	83	78	141	198	348	17	18	116	248	419	715	1986
20	2	8	46	42	253	270	856	1040	9	56	31	62	459	537	19
21	0	2	24	58	124	439	235	779	20	9	127	26	468	722	266
22	1	11	33	24	143	333	134	476	18	11	98	140	209	37	471
23	2	11	18	25	63	399	542	191	31	23	23	121	311	488	1166
24	1	3	37	92	41	14	545	1393	13	8	38	12	211	179	1300
25	2	15	35	38	214	277	777	1752	2	7	18	41	510	430	1033
26	3	13	21	120	70	412	483	1627	18	24	62	249	320	264	1606

3.4 ENCODING

The recommended method for producing codeblocks consistent with AR4JA parity-check matrices is to perform matrix multiplication by block-circulant generator matrices. Note that the family of AR4JA codes supports rates $K/(K+2)$, where K=2 for a rate 1/2 code, K=4 for rate 2/3, and K=8 for rate 4/5. AR4JA generator matrices, G, have size $MK \times M(K+3)$ if punctured columns are described in the encoding, or $MK \times M(K+2)$ if punctured columns are omitted. These matrices may be constructed as follows.

1) Let P be the $3M \times 3M$ submatrix of H consisting of the last $3M$ columns. Let Q be the $3M \times MK$ submatrix of H consisting of the first MK columns.

2) Compute $W = (P^{-1}Q)^T$, where the arithmetic is performed modulo-2.

3) Construct the matrix $G = [I_{MK} \quad W]$, where I_{MK} is the $MK \times MK$ identity matrix, and W is a dense matrix of circulants of size $MK \times M(N\text{-}K)$. Note that we can define N such that code block size is $n_{unpunc} = MN$. For AR4JA codes, n_{unpunc} also equals $M(K+3)$ [1]. We can then therefore express the dimension of W as $MK \times 3M$, or $MK \times 2M$ in the case where punctured variables are omitted from the generator matrix.

The matrix G is block-circulant and is composed of sets of superimposed size $m = M/4$ circulants. These superimposed block-circulants have a compact description based on the summation of monomials of the form x^i ($i \in \{0,\ldots,m\text{-}1\}$) where x^i represents a circulant matrix with a one in the ith column of the first row (row $j = 0$), the $i+1$th column of the second row (row $j = 1$), and the $((i+j) \bmod m)$th row of the jth column. Note that block circulant x^0 is the identity matrix.

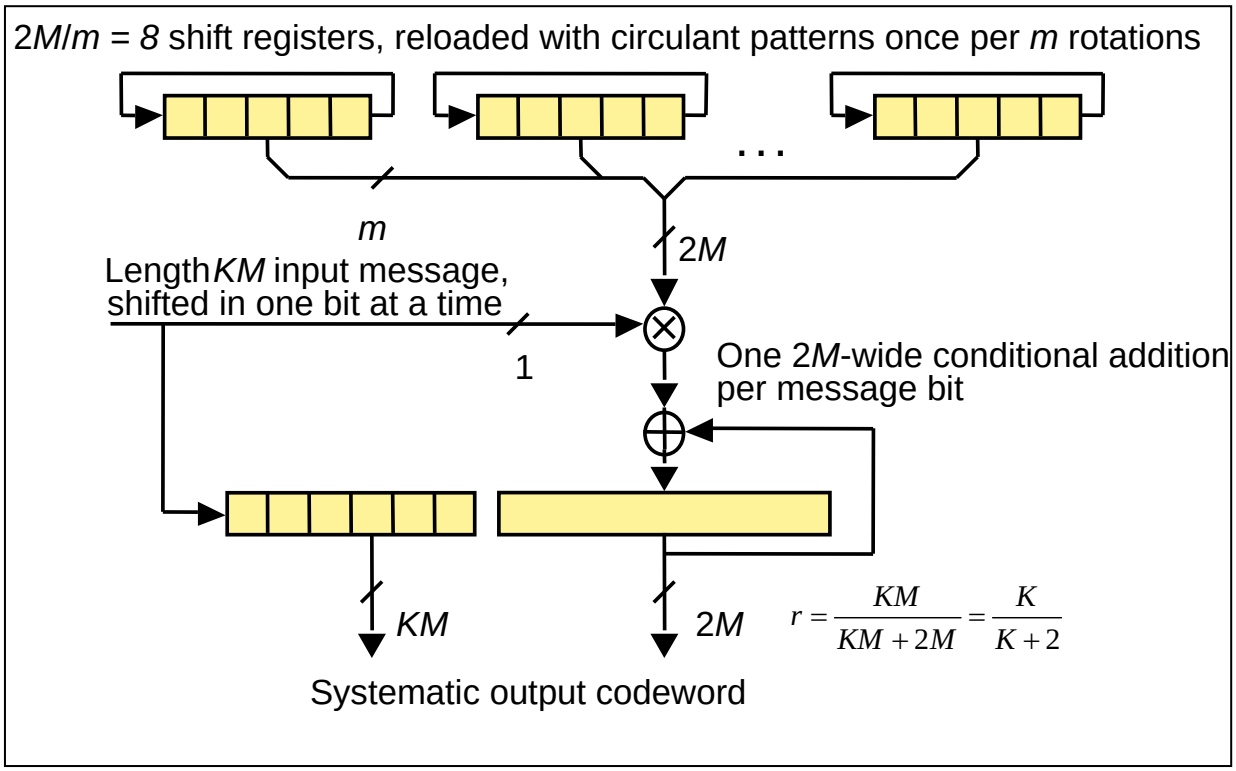

Figure 3-2: A Quasi-Cyclic Encoder Using Feedback Shift Registers

[1] We distinguish n_{unpunc}, the total number of codesymbols in the parity-check matrix of an AR4JA code, from n, the number of transmitted codesymbols. Note that $n = M(K+2)$.

Table 3-5: Description of Rate 4/5 k = 1024 Quasi-Cyclic Encoding. Degree-32 Parity Generation Polynomials Expressed As Hexadecimal Characters (Punctured Columns are Omitted)

	Col							
Row	0,31	32,63	64,95	96,127	128,159	160,191	192,223	224,255
0,31	8AD371E6	3AB8417F	D242FA5F	55E49AAF	C896417C	30D2074C	D46111F2	F74C2C01
32,63	A46E4D42	8785B1F9	D8B4E21F	29CBC29B	AEA86494	1632C25D	592CF718	233853E4
64,95	E9C00937	C6052526	652373D9	F0E5DA0B	87DAA8E7	83390FFE	9A047476	A7E6A8FE
96,127	3808686A	D4706057	D160CE6D	D1FBDC49	BC2C9D9D	15C63920	7F397CCC	B46CD901
128,159	32C682B9	5BE87202	4F8682DC	7499AC4A	D1D2D257	873D0962	856C5B9F	8DD9C268
160,191	AD2A4EBA	D1E92DA8	244A0B00	209BDE08	1A7EBA13	A58F8A20	E918B977	9F65BC89
192,223	86F98142	53CEEC2C	54926588	FC2F4C12	B7883921	F2617F0F	0020E433	766B64E9
224,255	22547791	E6F83A16	68276FB8	F74FDE0A	DF439AE1	FD54684A	DFCB86D4	2310E119
256,287	9057F152	2AC4A2CA	CE747CC5	884178E4	A746FB68	2F81FBC0	F0BD1211	EACFBA9F
288,319	CDE507D9	D76A4E86	2DD0B259	985C5C7F	79BC655F	18914CA6	AC5D996B	07F67B32
320,351	A7F8D121	F651AD50	8FE0E82C	D2E26CF7	A5E5C46F	5D937AC5	76D90924	1915E526
352,383	75DCFBBD	645F404E	EA309F61	04F99C05	8C59D4E9	75A24DE1	1CC5A307	9B559A92
384,415	E4364EF3	59421CDE	2243EC5D	DBE8EE77	53993A27	DC807C7E	253001DE	E74FE4A6
416,447	41EC63AE	EC802338	68F9678A	FAA8D282	7B2698FB	EF8E3C8F	22017976	61373A36
448,479	1FB654F6	41FD4FF9	AACA46CB	81966224	83528FAB	57524387	C1B0A115	048A3C5E
480,511	C3B5D55D	B660F378	12C1CA6E	2AB2BA3F	F362B5C2	348042CC	3B47D7C6	71F74C1B
512,543	8F413767	41E7F552	1C791B28	402C13C4	FD6B12D1	591DC413	646AC516	8487F917
544,575	8CC55DD2	93683704	607D5B56	B65BC01B	82B9133F	1708DEA7	280FFC33	6042EDB2
576,607	61ABFC0A	89D16F4A	CFB96BE9	726E3948	EFC284D1	5DCF76C5	3691E43E	ADE6F06A
608,639	6709C0EB	57ECCD19	C6C16A91	FB816854	314972D2	39BC3782	4D749BFB	3A13ABA5
640,671	BD110A54	0816D36E	84BC96D3	ABF79703	760A499F	41073994	65AA8809	6855C9D0
672,703	737F7F18	6CAC600D	910E12A9	9DD8CDD2	E9BFCF66	051AD4C7	5E429C54	F97B1B3A
704,735	6861F158	4D4BEFA3	723D4B5A	DB6178FD	5FFDEF35	E9A91ACF	32A6EEE5	26C8BB48
736,767	9A5C03FF	E4A0A23B	8E132DCC	CC57455D	658AE5C9	B274EB9F	FE30AD96	9F8A82EF
768,799	B98A17DE	5F5FF6F5	CE5DB164	31486AC5	347D1820	5A62C258	A6FB6306	051C2470
800,831	A03BA437	15277566	50C054E5	086DF88D	EF5B2EBB	A6AB6F46	ED7572AA	3675EFA8
832,863	509FE28A	803770FF	36699548	8DA0E8E1	0CFFAC97	EA94C762	3F96B62A	60BD851D
864,895	F6570156	60A9458E	F3551EF7	B7AD4AB1	669250F9	716DCD86	69F5E8D2	743414DA
896,927	4E441AAE	9942A768	39D0E0BE	EA80C8D5	4B98636E	AB4700AA	9A2019F8	C1FE39BA
928,959	B85BB056	086D176F	85070BA4	0792E424	60525B7F	6B96B4E0	9E5BE3C0	AACC558A
960,991	0FF7F976	8FD3E9E0	24136C97	AF578393	627E062B	70DEB711	B5068749	B50288CE
992,1023	F53F7F4C	AEDC610E	088F621C	FFBC4723	CAEFCB9E	5F126260	AF4A20C1	A221B79D

As an example, table 3-5 lists every $M/4$'th row of W (the first row of each set of circulants) for the generator matrix of the (n = 1280, k = 1024) rate 4/5 code. For this code (M = 128, K = 8) therefore block-circulants have size $M/4 = m = 32$. The table dimensions are MK/m = 1024/32 = 32 rows and $2M/m$ = 8 columns of summed monomials (polynomials) of degree up to m-1 = 31 (Note that the last M columns for the punctured symbols are not included). Rather than writing long polynomials into the table, we have instead used hexadecimal notation. For example the (1,1) element (`0x8AD371E6`) denotes polynomial $x^{31} + x^{27} + x^{25} +$

$x^{23} + x^{22} + x^{20} + x^{17} + x^{16} + x^{14} + x^{13} + x^{12} + x^{8} + x^{7} + x^{6} + x^{5} + x^{2} + x^{1}$. A procedure for deriving AR4JA encoding matrices can be found in annex B.

Encoding of message m requires computing mG. Because G is block-circulant, this can be performed in an efficient bit-serial manner using $2M/m = 8$ (for all rates) linear feedback shift registers, each of length $m = M/4$, as shown in figure 3-2. Initially, the binary pattern from the first row of circulants (or first row of table 3-5) is placed in the shift registers. Correct endianess occurs if higher order monomials (leftmost hexadecimal digits) are placed closer to the output than the input of each shift register. Also, in terms of mG, the first bit to be encoded by the circuit represents the bit in the leftmost element of row vector m. After m bit arrivals (and cyclic shifts) then next row of circulants (second row of table 3-5) is loaded. Encoding is complete after MK/m rows of circulants have been loaded. Each requires m clock cycles to process for a total of $k = MK$ clock cycles to compute the parity for one codeword. Many architectural alternatives are possible. The main benefits of the architecture in figure 3-2 are conceptual simplicity and relatively high throughput (n codeword bits are computed in k clock cycles).

3.5 SYNCHRONIZATION

Codeblock synchronization is achieved by synchronization of an Attached Sync Marker associated with each LDPC Codeblock. The Attached Sync Marker (ASM) is a bit pattern specified in section 6 of CCSDS Recommended Standard CCSDS 131.0-B-1, *TM Synchronization and Channel Coding* (reference [1]), as an aid to synchronization, and it precedes the LDPC Codeblock. Frame synchronizers should be set to expect a marker at a recurrence interval equal to the length of the ASM plus that of the LDPC Codeblock. All codes in the LDPC family use the 64-bit ASM.

ANNEX A

ANNEX TO SECTION 2, LOW DENSITY PARITY CHECK CODE OPTIMIZED FOR NEAR-EARTH APPLICATIONS

A1 GENERATOR MATRIX CIRCULANT TABLE

Table A-1: Table of Circulants for the Generator Matrix

Circulant	1st row of circulant
$B_{1,1}$	55BF56CC55283DFEEFEA8C8CFF04E1EBD9067710988E25048D67525426939E206 8D2DC6FCD2F822BEB6BD96C8A76F4932AAE9BC53AD20A2A9C86BB461E43759C
$B_{1,2}$	6855AE08698A50AA3051768793DC238544AF3FE987391021AAF6383A6503409C3C E971A80B3ECE12363EE809A01D91204F1811123EAB867D3E40E8C652585D28
$B_{2,1}$	62B21CF0AEE0649FA67B7D0EA6551C1CD194CA77501E0FCF8C85867B9CF679C18B CF7939E10F8550661848A4E0A9E9EDB7DAB9EDABA18C168C8E28AACDDEAB1E
$B_{2,2}$	64B71F486AD57125660C4512247B229F0017BA649C6C11148FB00B70808286F1A97 90748D296A593FA4FD2C6D7AAF7750F0C71B31AEE5B400C7F5D73AAF00710
$B_{3,1}$	681A8E51420BD8294ECE13E491D618083FFBBA830DB5FAF330209877D801F92B5 E07117C57E75F6F0D873B3E520F21EAFD78C1612C6228111A369D5790F5929A
$B_{3,2}$	04DF1DD77F1C20C1FB570D7DD7A1219EAECEA4B2877282651B0FFE713DF338A6 3263BC0E324A87E2DC1AD64C9F10AAA585ED6905946EE167A73CF04AD2AF9218
$B_{4,1}$	35951FEE6F20C902296C9488003345E6C5526C5519230454C556B8A04FC0DC642D 682D94B4594B5197037DF15B5817B26F16D0A3302C09383412822F6D2B234E
$B_{4,2}$	7681CF7F278380E28F1262B22F40BF3405BFB92311A8A34D084C086464777431DBF DDD2E82A2E6742BAD6533B51B2BDEE0377E9F6E63DCA0B0F1DF97E73D5CD8
$B_{5,1}$	188157AE41830744BAE0ADA6295E08B79A44081E111F69BBE7831D07BEEBF76232 E065F752D4F218D39B6C5BF20AE5B8FF172A7F1F680E6BF5AAC3C4343736C2
$B_{5,2}$	5D80A6007C175B5C0DD88A442440E2C29C6A136BBCE0D95A58A83B48CA0E7474 E9476C92E33D164BFF943A61CE1031DFF441B0B175209B498394F4794644392E
$B_{6,1}$	60CD1F1C282A1612657E8C7C1420332CA245C0756F78744C807966C3E132643887 8BD2CCC83388415A612705AB192B3512EEF0D95248F7B73E5B0F412BF76DB4
$B_{6,2}$	434B697B98C9F3E48502C8DBD891D0A0386996146DEBEF11D4B833033E05EDC28 F808F25E8F314135E6675B7608B66F7FF3392308242930025DDC4BB65CD7B6E
$B_{7,1}$	766855125CFDC804DAF8DBE3660E8686420230ED4E049DF11D82E357C54FE256E A01F5681D95544C7A1E32B7C30A8E6CF5D0869E754FFDE6AEFA6D7BE8F1B148
$B_{7,2}$	222975D325A487FE560A6D146311578D9C5501D28BC0A1FB48C9BDA173E869133 A3AA9506C42AE9F466E85611FC5F8F74E439638D66D2F00C682987A96D8887C
$B_{8,1}$	14B5F98E8D55FC8E9B4EE453C6963E052147A857AC1E08675D99A308E7269FAC5 600D7B155DE8CB1BAC786F45B46B523073692DE745FDF10724DDA38FD093B1C

Circulant	1st row of circulant
$B_{8,2}$	1B71AFFB8117BCF8B5D002A99FEEA49503C0359B056963FE5271140E626F6F8FC E9F29B37047F9CA89EBCE760405C6277F329065DF21AB3B779AB3E8C8955400
$B_{9,1}$	0008B4E899E5F7E692BDCE69CE3FAD997183CFAEB2785D0C3D9CAE510316D4BD 65A2A06CBA7F4E4C4A80839ACA81012343648EEA8DBBA2464A68E115AB3F4034
$B_{9,2}$	5B7FE6808A10EA42FEF0ED9B41920F82023085C106FBBC1F56B567A14257021BC5 FDA60CBA05B08FAD6DC3B0410295884C7CCDE0E56347D649DE6DDCEEB0C95E
$B_{10,1}$	5E9B2B33EF82D0E64AA2226D6A0ADCD179D5932EE1CF401B336449D0FF775754C A56650716E61A43F963D59865C7F017F53830514306649822CAA72C152F6EB2
$B_{10,2}$	2CD8140C8A37DE0D0261259F63AA2A420A8F81FECB661DBA5C62DF6C817B4A61 D2BC1F068A50DFD0EA8FE1BD387601062E2276A4987A19A70B460C54F215E184
$B_{11,1}$	06F1FF249192F2EAF063488E267EEE994E7760995C4FA6FFA0E4241825A7F5B65C 74FB16AC4C891BC008D33AD4FF97523EE5BD14126916E0502FF2F8E4A07FC2
$B_{11,2}$	65287840D00243278F41CE1156D1868F24E02F91D3A1886ACE906CE741662B40B4 EFDFB90F76C1ADD884D920AFA8B3427EEB84A759FA02E00635743F50B942F0
$B_{12,1}$	4109DA2A24E41B1F375645229981D4B7E88C36A12DAB64E91C764CC43CCEC188E C8C5855C8FF488BB91003602BEF43DBEC4A621048906A2CDC5DBD4103431DB8
$B_{12,2}$	2185E3BC7076BA51AAD6B199C8C60BCD70E8245B874927136E6D8DD527DF0693 DC10A1C8E51B5BE93FF7538FA138B335738F4315361ABF8C73BF40593AE22BE4
$B_{13,1}$	228845775A262505B47288E065B23B4A6D78AFBDDB2356B392C692EF56A35AB4A A27767DE72F058C6484457C95A8CCDD0EF225ABA56B7657B7F0E947DC17F972
$B_{13,2}$	2630C6F79878E50CF5ABD353A6ED80BEACC7169179EA57435E44411BC7D566136 DFA983019F3443DE8E4C60940BC4E31DCEAD514D755AF95A622585D69572692
$B_{14,1}$	7273E8342918E097B1C1F5FEF32A150AEF5E11184782B5BD5A1D8071E94578B0AC 722D7BF49E8C78D391294371FFBA7B88FABF8CC03A62B940CE60D669DFB7B6
$B_{14,2}$	087EA12042793307045B283D7305E93D8F74725034E77D25D3FF043ADC5F8B5B18 6DB70A968A816835EFB575952EAE7EA4E76DF0D5F097590E1A2A978025573E

Note that the numbers in the second column represent the hexadecimal representation of the first row of each circulant. Since there are only 511 possible positions, the leftmost bit is padded with a zero to allow a 128 digit hexadecimal number. Table A-1 cannot be as efficiently described as table 2-5 because the generator circulants do not have a low density of '1's.

A2 COMPLEXITY

The complexity of LDPC codes has been an area of research and discussion. For a Field Programmable Gate Array (FPGA) or Application Specific Integrated Circuit (ASIC) implementation, the encoder's complexity are dominated by two factors: 1) the total number of required logic gates and 2) the routing complexity. For the code presented in this Experimental Specification, the quasi-cyclic property allows for the use of shift registers whose required number of logic gates is proportional to $n–k$ (see reference [C1.6]) or 8176–7156 = 1020 (unshortened). With regard to the routing complexity, there is currently no way

to predict this figure: it would depend on a number of factors, such as the choice of the FPGA or ASIC, the routing algorithm, and the layout of the device.

The decoder's complexity is larger than the encoder's and even more difficult to predict. The primary complexity factors (the total number of required logic gates and the routing complexity) are a function of the choice of BP decoding algorithm (there are many) as well as the architectural decisions (i.e., parallel or serial processing, number of bits of finite precision, fixed number of iterations or stopping rule, use of look-up tables, etc.) These choices also determine the decoder's Bit Error Rate (BER) performance.

For the development of the baselined (8176, 7156) code, an FPGA implementation was used to confirm the software simulations. A Xilinx 8000 Virtex-2 FPGA was used for the test. The device contained both the encoder and decoder. The decoder algorithm was a Scaled Min-Sum Parallel BP Decoder (SMSPD) described in reference [C1.7]. The encoder algorithm was a shift register based encoder described in reference [C1.6]. An architectural evaluation was performed prior to implementation to produce a quasi-optimal implementation based on routing, logic requirements, and BER performance.

The FPGA had the following statistics:

1) encoder used 2,535 logic slices out of 46,592 available or 5.4% and 4 memory blocks out of 168 available or 2.4%;

2) decoder used 21,803 logic slices out of 46,592 or 46.8% and 137 memory blocks out of 168 or 81.5%.

The number of logic slices is an aggregate measure of the number of logic gates required and the routing complexity, while the memory blocks figure is the number of dedicated FPGA memory blocks used. It is clear from these statistics that the encoder is of much lower complexity than the decoder, using only 5.4% of the logic slices resources while the decoder requires 46%.

Annex A3 summarizes the test results.

A3 FPGA TEST RESULTS

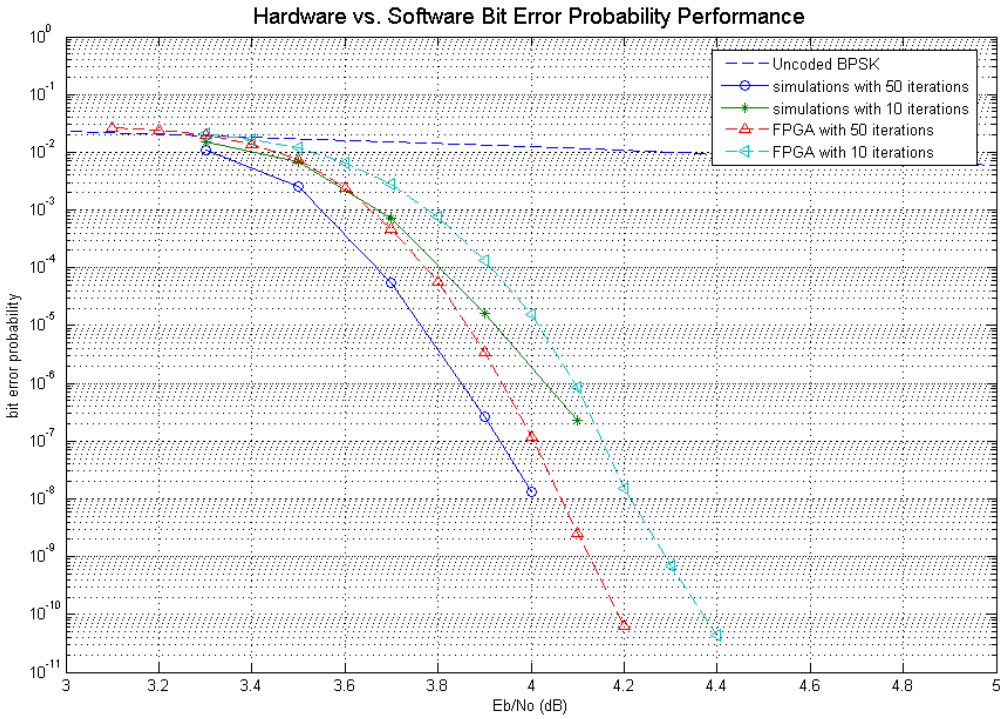

Figure A-1: Bit Error Rate Test Results

Figure A-1 shows the BER and figure A-2 shows the Block Error Rate (BLER) test results for 50 and 10 maximum iterations from an FPGA implementation of the baselined (8176, 7156) code. Note that for both cases the difference between simulations and hardware tests was 0.1 dB or less.

The encoder data rate was limited to 2 × system clock while the decoder operated at 14 × system clock / number of iterations. For testing, the system clock was set to 100 MHz, so for 10 iterations, the decoder operated at 140 Mbps. Although the shortened (8160, 7136) was not tested, it is reasonable to say that the baselined (8176, 7156) and the shortened (8160, 7136) codes will have similar results.

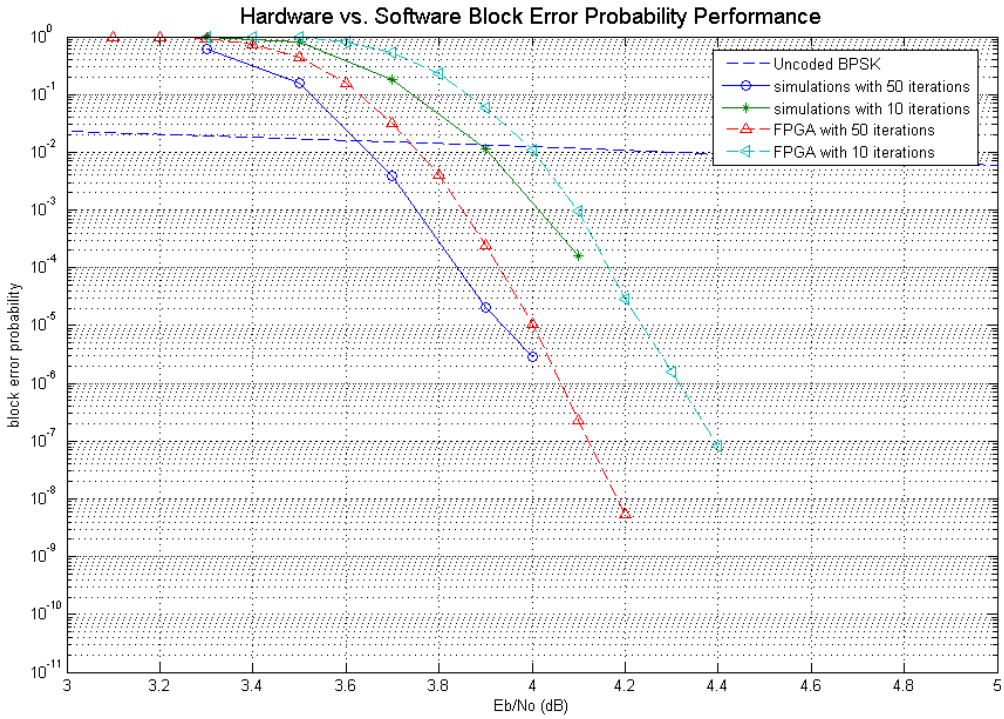

Figure A-2: Block Error Rate Test Results

ANNEX B

ANNEX TO SECTION 3, LOW DENSITY PARITY CHECK CODE FAMILY OPTIMIZED FOR DEEP SPACE APPLICATIONS

B1 COMPUTATION OF DENSE GENERATOR SUBMATRIX W

To clarify the procedure for computing *W* (from section 3.4), we describe a step-by-step method for finding the generator matrix for a rate 1/2 AR4JA LDPC code with very short block length (*k* = 32). Consider the protograph of the rate 1/2 AR4JA LDPC code shown in figure B-1

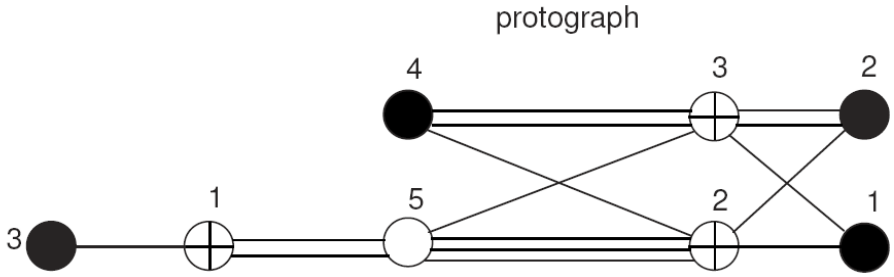

Figure B-1: Protograph for Rate 1/2 AR4JA LDPC Code

Expand the protograph by a factor of 4 to remove parallel edges. Assign circulant permutations to edges on the expanded graph. The expanded protograph has the following *H* matrix.

$$H = \begin{bmatrix}
0 & 0 & 0 & 0 & 0 & 0 & 0 & 0 & 1 & 0 & 0 & 0 & 0 & 0 & 0 & 0 & 1 & 0 & 0 & x^1 \\
0 & 0 & 0 & 0 & 0 & 0 & 0 & 0 & 0 & 1 & 0 & 0 & 0 & 0 & 0 & 0 & 1 & 1 & 0 & 0 \\
0 & 0 & 0 & 0 & 0 & 0 & 0 & 0 & 0 & 0 & 1 & 0 & 0 & 0 & 0 & 0 & 0 & 1 & 1 & 0 \\
0 & 0 & 0 & 0 & 0 & 0 & 0 & 0 & 0 & 0 & 0 & 1 & 0 & 0 & 0 & 0 & 0 & 0 & 1 & 1 \\
1 & 0 & 0 & 0 & 1 & 0 & 0 & 0 & 0 & 0 & 0 & 0 & 1 & 0 & 0 & 0 & x^2 & x^2 & x^2 & 0 \\
0 & 1 & 0 & 0 & 0 & 1 & 0 & 0 & 0 & 0 & 0 & 0 & 0 & 1 & 0 & 0 & 0 & x^0 & x^0 & x^3 \\
0 & 0 & 1 & 0 & 0 & 0 & 1 & 0 & 0 & 0 & 0 & 0 & 0 & 0 & 1 & 0 & x^2 & 0 & x^3 & x^1 \\
0 & 0 & 0 & 1 & 0 & 0 & 0 & 1 & 0 & 0 & 0 & 0 & 0 & 0 & 0 & 1 & x^2 & x^2 & 0 & x^2 \\
1 & 0 & 0 & 0 & 0 & 0 & x^3 & x^2 & 0 & 0 & 0 & 0 & x^3 & x^3 & 0 & 0 & 1 & 0 & 0 & 0 \\
0 & 1 & 0 & 0 & x^0 & 0 & 0 & 1 & 0 & 0 & 0 & 0 & 0 & x^3 & x^3 & 0 & 0 & 1 & 0 & 0 \\
0 & 0 & 1 & 0 & x^3 & x^0 & 0 & 0 & 0 & 0 & 0 & 0 & 0 & 0 & x^3 & 1 & 0 & 0 & 1 & 0 \\
0 & 0 & 0 & 1 & 0 & x^0 & x^2 & 0 & 0 & 0 & 0 & 0 & x^1 & 0 & 0 & x^2 & 0 & 0 & 0 & 1
\end{bmatrix}$$

The first 4 rows correspond to check node number 1 in figure B-1, the second 4 rows and the last 4 rows correspond to check nodes 2 and 3, respectively. The first 4 columns correspond to variable node number 1 in figure B-1. The subsequent 4 groups of 4 columns correspond to variable node numbers 2, 3, 4 and 5 respectively in figure B-1. For this example $M = 16$ and the $m \times m$ circulant permutations have size $m = 4$. Each nonzero entry x^i in the parity check matrix H represents a circulant permutation (an $m \times m$ identity matrix where each row is circularly shifted to the right by i).

All operations are over the ring of polynomials with coefficients in GF(2) modulo x^m+1.

Step 1 : Denote the first 8 columns of H as Q, and the last 12 columns as P:

$$Q = \begin{bmatrix} 0 & 0 & 0 & 0 & 0 & 0 & 0 & 0 \\ 0 & 0 & 0 & 0 & 0 & 0 & 0 & 0 \\ 0 & 0 & 0 & 0 & 0 & 0 & 0 & 0 \\ 0 & 0 & 0 & 0 & 0 & 0 & 0 & 0 \\ 1 & 0 & 0 & 0 & 1 & 0 & 0 & 0 \\ 0 & 1 & 0 & 0 & 0 & 1 & 0 & 0 \\ 0 & 0 & 1 & 0 & 0 & 0 & 1 & 0 \\ 0 & 0 & 0 & 1 & 0 & 0 & 0 & 1 \\ 1 & 0 & 0 & 0 & 0 & 0 & x^3 & x^2 \\ 0 & 1 & 0 & 0 & x^0 & 0 & 0 & 1 \\ 0 & 0 & 1 & 0 & x^3 & x^0 & 0 & 0 \\ 0 & 0 & 0 & 1 & 0 & x^0 & x^2 & 0 \end{bmatrix}$$

$$P = \begin{bmatrix} 1 & 0 & 0 & 0 & 0 & 0 & 0 & 0 & 1 & 0 & 0 & x^1 \\ 0 & 1 & 0 & 0 & 0 & 0 & 0 & 0 & 1 & 1 & 0 & 0 \\ 0 & 0 & 1 & 0 & 0 & 0 & 0 & 0 & 0 & 1 & 1 & 0 \\ 0 & 0 & 0 & 1 & 0 & 0 & 0 & 0 & 0 & 0 & 1 & 1 \\ 0 & 0 & 0 & 0 & 1 & 0 & 0 & 0 & x^2 & x^2 & x^2 & 0 \\ 0 & 0 & 0 & 0 & 0 & 1 & 0 & 0 & 0 & x^0 & x^0 & x^3 \\ 0 & 0 & 0 & 0 & 0 & 0 & 1 & 0 & x^2 & 0 & x^3 & x^1 \\ 0 & 0 & 0 & 0 & 0 & 0 & 0 & 1 & x^2 & x^2 & 0 & x^2 \\ 0 & 0 & 0 & 0 & x^3 & x^3 & 0 & 0 & 1 & 0 & 0 & 0 \\ 0 & 0 & 0 & 0 & 0 & x^3 & x^3 & 0 & 0 & 1 & 0 & 0 \\ 0 & 0 & 0 & 0 & 0 & 0 & x^3 & 1 & 0 & 0 & 1 & 0 \\ 0 & 0 & 0 & 0 & x^1 & 0 & 0 & x^2 & 0 & 0 & 0 & 1 \end{bmatrix}$$

Step 2 : Find the cofactor matrix of P and denote it P_c. This is the transpose of the matrix composed of determinants of all sub-matrices of P found by eliminating each row/column pair and forming a matrix from each set of remaining elements.

Step 3 : Find the determinant of P, denote it by polynomial $d(x)$.

In this example $d(x) = x+x^2+x^3$.

Step 4 : Find the inverse of polynomial $d(x)$ using Euclid's algorithm.

In this example $d^{-1}(x) = x+x^2+x^3$

Step 5 : Multiply to find $P_i = d^{-1}(x)P_c$

Step 6 : Multiply to find $W_2 = (P_iQ)^T$

Step 7: Find the reciprocal polynomial of each entry of W_2 and denote the result W. This step serves to swap row / column ordering of all circulants in W_2.

Step 8: We then obtain the generator matrix $G = [I_{MK}\ W]$

$$W_P = \begin{bmatrix} 1+x^2 & x^2+x^3 & 1 & x & 1+x^3 & x^3 & 1+x+x^2 & 0 \\ 1+x^2+x^3 & 1+x & 1+x^2 & x^3 & x+x^2 & 0 & 1+x+x^2 & x^2 \\ 1+x^2+x^3 & x+x^2+x^3 & x+x^2 & 0 & 1+x^2+x^3 & 1+x^2 & x+x^3 & 1+x^2+x^3 \\ 1+x & x & 1+x+x^2 & x+x^2 & x+x^2+x^3 & x^3 & 1+x+x^2+x^3 & x+x^2 \\ 0 & x^2+x^3 & 0 & x+x^3 & 1+x^3 & x^3 & 1+x+x^2 & x \\ x^2+x^3 & 1+x & 1+x^2 & 1+x & x^2 & x+x^2 & 1+x^2+x^3 & x^3 \\ x+x^2 & x+x^3 & 1+x^3 & x^2+x^3 & 1+x^2+x^3 & 1+x+x^3 & 1+x^3 & x+x^2+x^3 \\ x^2+x^3 & 0 & 0 & 1+x+x^2+x^3 & x^3 & 1+x+x^3 & x & x+x^2 \end{bmatrix}$$

The most compact representation of an encoding omits punctured columns as well as the leading I_{MK} identity matrix. We denote such a representation as W_p and express the W_p embedded within the G of Step 8 using hexadecimal digits as:

$$W_P = \begin{bmatrix} 5 & C & 1 & 2 & 9 & 8 & 7 & 0 \\ D & 3 & 5 & 8 & 6 & 0 & 7 & 4 \\ D & E & 6 & 0 & D & 5 & A & D \\ 3 & 2 & 7 & 6 & E & 8 & F & 6 \\ 0 & C & 0 & A & 9 & 8 & 7 & 2 \\ C & 3 & 5 & 3 & 4 & 6 & D & 8 \\ 6 & A & 9 & C & D & B & 9 & E \\ C & 0 & 0 & F & 8 & B & 2 & 6 \end{bmatrix}$$

B2 PERFORMANCE

Figure B-2 shows the frame error rates (dashed) and symbol error rates (solid) for the short blocklength members of the code family. From left to right, these three codes have parameters (n=2048, k=1024) rate 1/2, (n=1536, k=1024) rate 2/3, and (n=1280,k=1024) rate 4/5. Similarly, figure B-3 shows performance curves for the midsize blocklength codes with parameters (n=8192, k=4096) rate 1/2, (n=6144, k=4096) rate 2/3, and (n=5120, k=4096) rate 4/5. Figure B-4 shows performance curves for the long blocklength codes with parameters (n=32768, k=16384) rate 1/2, (n=24576, k=16384) rate 2/3, and (n=20480, k=16384) rate 4/5. Finally, figure B-5 provides a composite plot of the performance of all nine AR4JA codes.

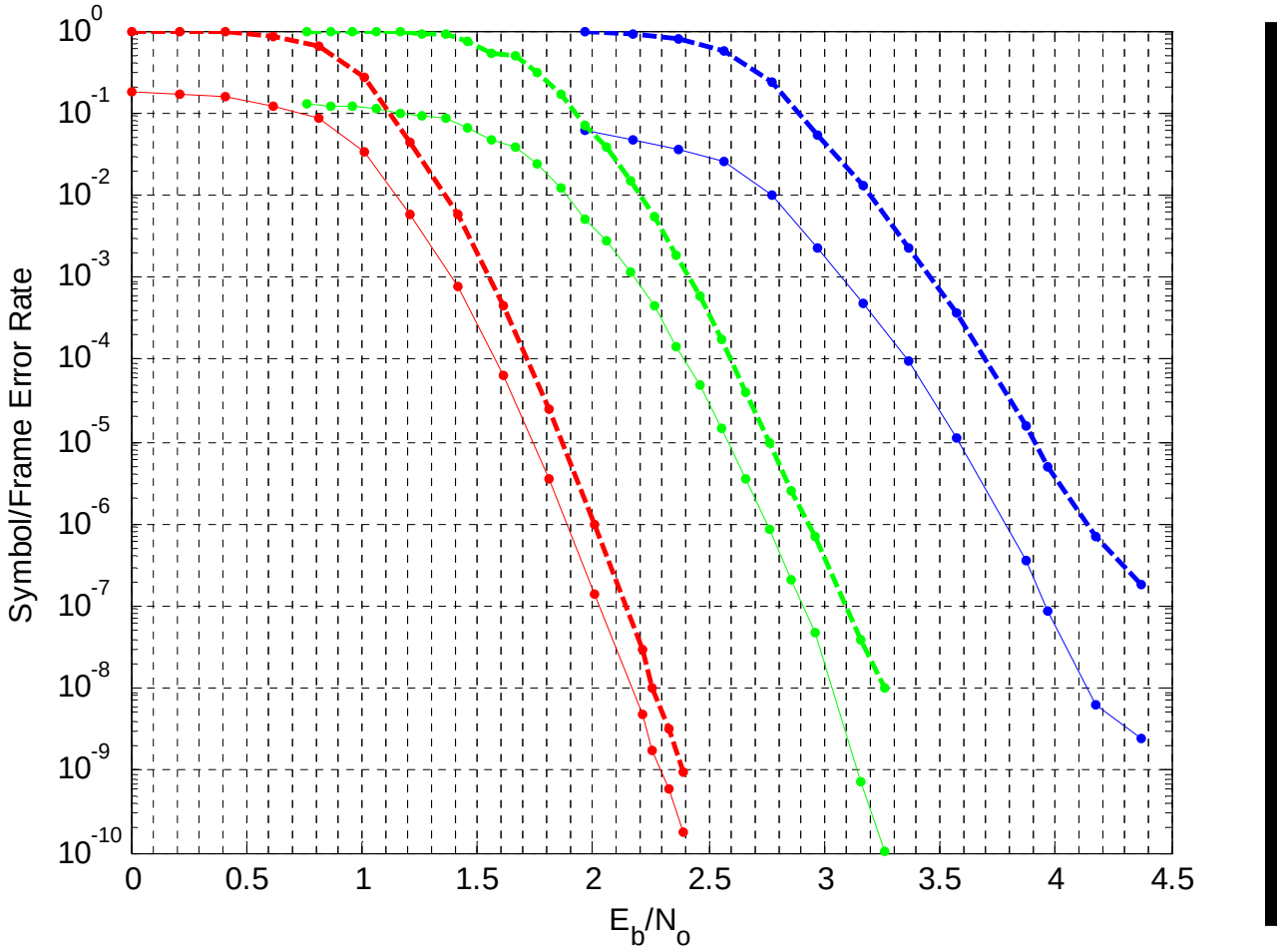

Figure B-2: Performance of Length *k*=1024 LDPC Codes: Rate 1/2, 2/3, 4/5 (Left to Right)

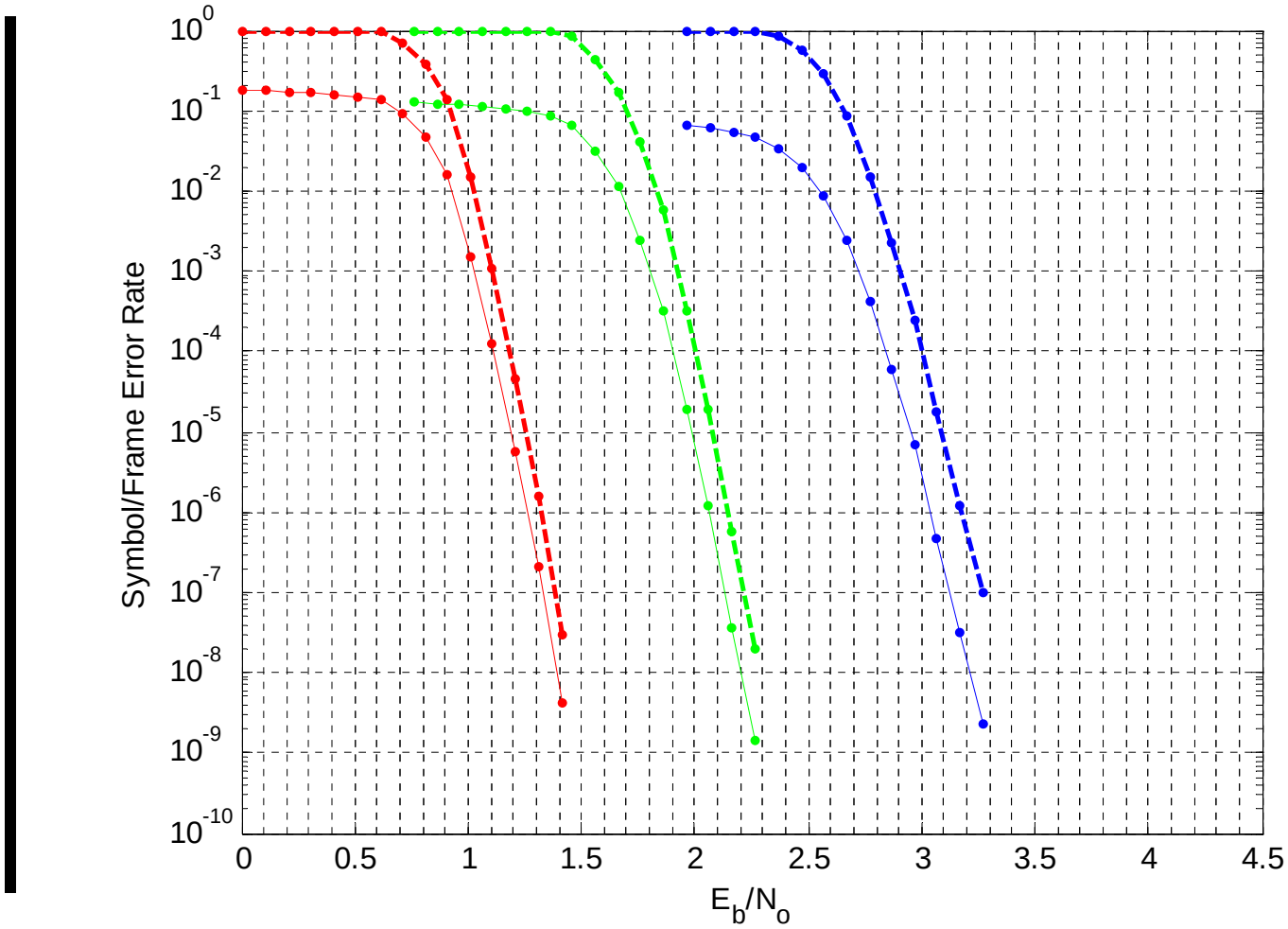

Figure B-3: Performance of Length *k*=4096 LDPC Codes: Rate 1/2, 2/3, 4/5 (Left to Right)

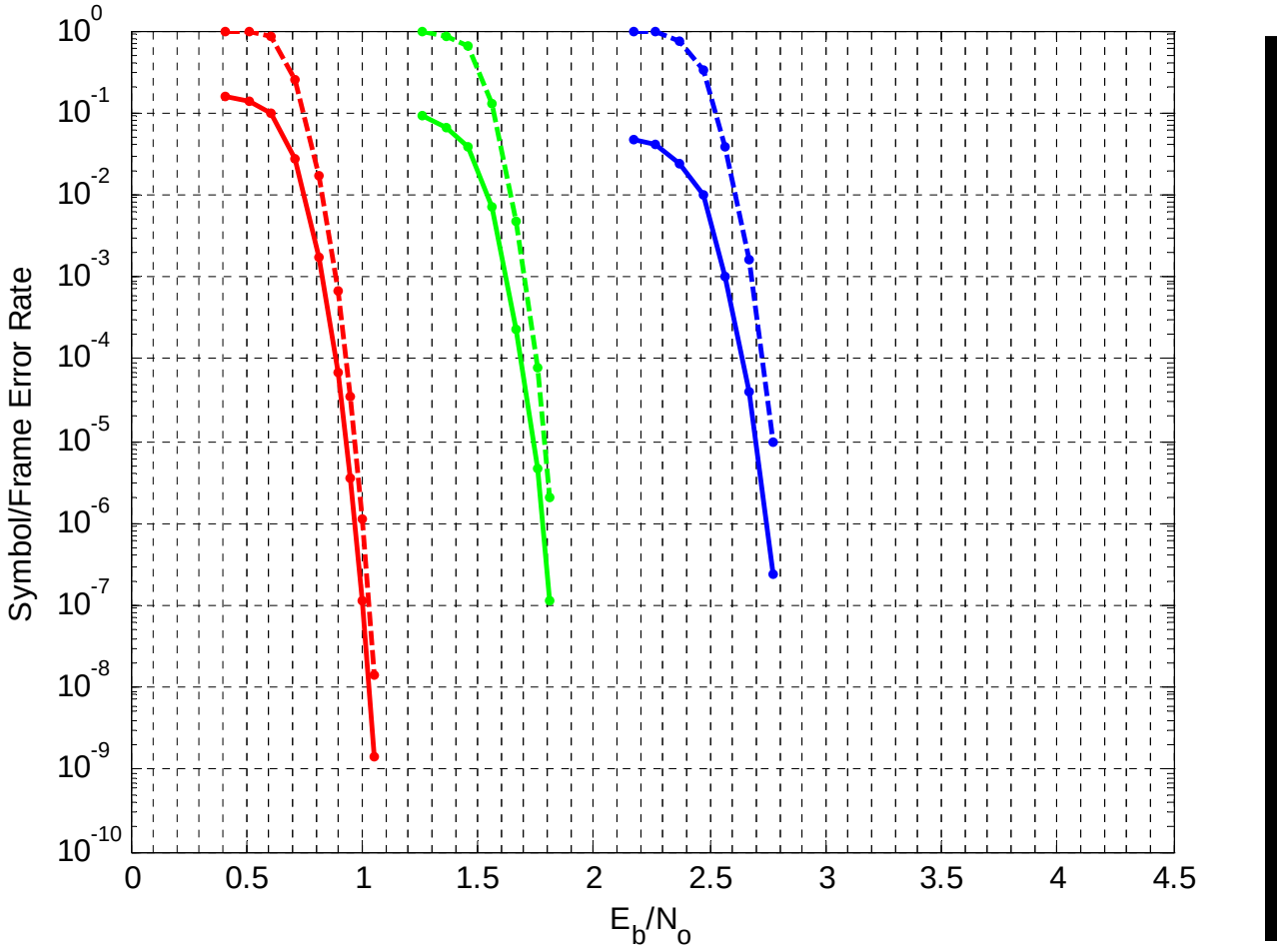

Figure B-4: Performance of Length *k*=16384 LDPC Codes: Rate 1/2, 2/3, 4/5 (Left to Right)

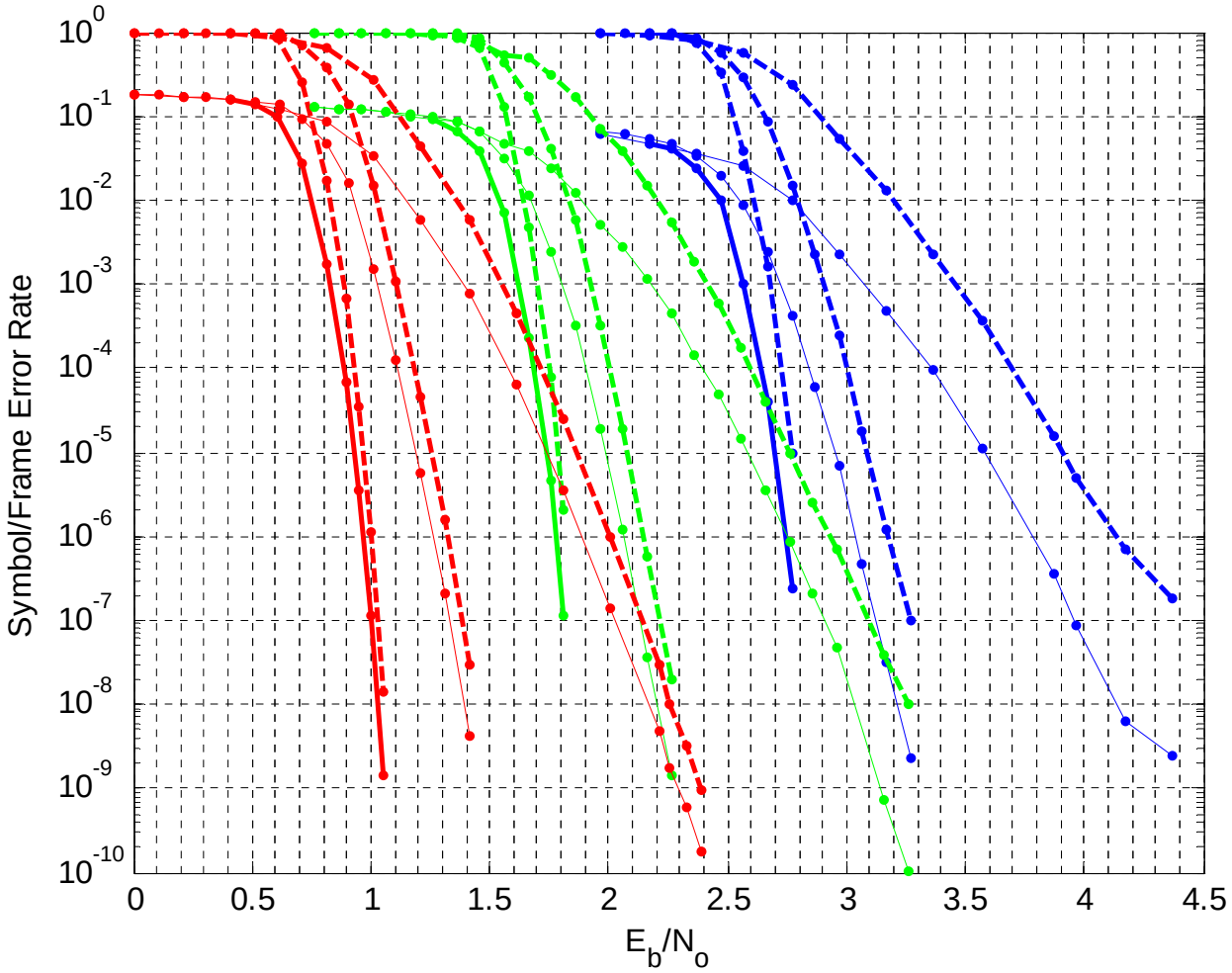

Figure B-5: Performance of Length *k*=16384, *k*=4096, *k*=1024 AR4JA LDPC Codes: Rate 1/2 (Red), 2/3 (Green), 4/5 (Blue)

Performance curves for the codes with k = 1024 and k = 4096 were determined by hardware simulation on a Xilinx Virtex-II FPGA (see reference [C2.7]); performance for the k=16384 codes are from software simulations (except rate 1/2 performance which was also found via hardware simulation). In each case, a large maximum number of iterations was allowed, and a stopping rule was used so the average number of iterations required remained small.

It is well known that error floors can be caused either by the structure of the code, or by implementation details of the decoder. The error floor that appears above FER 10^{-7} for the (n=1280, k=1024) rate 4/5 code may be due in part to characteristics of the decoders used.

ANNEX C

INFORMATIVE REFERENCES

C1 INFORMATIVE REFERENCES FOR SECTION 2, LOW DENSITY PARITY CHECK CODE OPTIMIZED FOR NEAR EARTH APPLICATIONS

[C1.1] D. J. C. MacKay and R. M. Neal. "Near Shannon Limit Performance of Low Density Parity Check Codes." *Electro. Lett.* 32 (August 1996): 1645-1646.

[C1.2] R. G. Gallager. "Low Density Parity Check Codes." *IRE Trans. Inform. Theory* IT-8 (January 1962): 21-28.

[C1.3] T. Richardson and R. Urbanke. "Design of Capacity-Approaching Low Density Parity Check Codes." *IEEE Trans. Inform. Theory* 47 (February 2001): 619-637.

[C1.4] Y. Kou, S. Lin, and M. P. C. Fossorier. "Low-Density Parity-Check Codes Based on Finite Geometries: A Rediscovery and New Results." *IEEE Trans. Information Theory* 47 (November 2001): 2711-2736.

[C1.5] W. Fong, "White Paper for Low Density Parity Check (LDPC) Codes for CCSDS Channel Coding Blue Book." CCSDS P1B Channel Coding Meeting, Houston, TX, October 2002.

[C1.6] Z. Li, et al. "Efficient Encoding of Quasi-Cyclic Low-Density Parity-Check Codes." *IEEE Transactions on Communications* 54, no. 1 (January 2006): 71-81.

[C1.7] J. Heo. "Analysis of Scaling Soft Information on Low Density Parity Check Code." *Electro. Lett.* 39 (January 2003): 219-221.

[C1.8] S. Lin and D. Costello, Jr. *Error Control Coding*. 2nd ed. New Jersey: Pearson Prentice Hall, 2004.

C2 INFORMATIVE REFERENCES FOR SECTION 3, LOW DENSITY PARITY CHECK CODE FAMILY OPTIMIZED FOR DEEP SPACE APPLICATIONS

[C2.1] D. Divsalar, S. Dolinar, and C. Jones. "Low-Rate LDPC Codes with Simple Protograph Structure." In *Proceedings of the IEEE International Symposium on Information Theory (Adelaide, Australia)*, 1622-1626. Piscataway, NJ: IEEE, September 2005.

[C2.2] D. Divsalar, S. Dolinar, and C. Jones. "Construction of Protograph LDPC Codes with Linear Minimum Distance." In *Proceedings of the IEEE International Symposium on Information Theory (Seattle, Washington)*. Piscataway, NJ: IEEE, July 2006.

[C2.3] A. Abbasfar, D. Divsalar, and K. Yao. "Accumulate Repeat Accumulate Codes." In *Proceedings of GLOBECOM '04 (Dallas, Texas)*, 1-509–1-513. Piscataway, NJ: IEEE, 29 Nov.-3 Dec. 2004.

[C2.4] K. Andrews, et al. "Design of Low-Density Parity-Check (LDPC) Codes for Deep Space Applications." *IPN Progress Report* 42-159 (November 2004). <http://tmo.jpl.nasa.gov/progress_report/42-159/159K.pdf>

[C2.5] K. Andrews, S. Dolinar, and J. Thorpe. "Encoders for Block-Circulant LDPC Codes." In *Proceedings of the IEEE International Symposium on Information Theory (Adelaide, Australia)*, 2300-2304. Piscataway, NJ: IEEE, September 2005.

[C2.6] S. Dolinar, D. Divsalar, and F. Pollara. "Code Performance as a Function of Block Size." *TMO Progress Report* 42-133 (January-March 1998). <http://tmo.jpl.nasa.gov/progress_report/42-159/159K.pdf>

[C2.7] C. Jones, et al. "Approximate-MIN* Constraint Node Updating for LDPC Code Decoding." In *Proceedings of MILCOM 2003 (Boston, Massachusetts)*, 1-157-1-162. Piscataway, NJ: IEEE, October 2003.

[C2.8] J. Lee and J. Thorpe. "Memory-Efficient Decoding of LDPC Codes." In Proceedings of the IEEE International Symposium on Information Theory (Adelaide, Australia), 459-463. Piscataway, NJ: IEEE, September 2005.

[C2.9] *TM Space Data Link Protocol*. Recommendation for Space Data System Standards, CCSDS 132.0-B-1. Blue Book. Issue 1. Washington, D.C.: CCSDS, September 2003.

[C2.10] *AOS Space Data Link Protocol*. Recommendation for Space Data System Standards, CCSDS 732.0-B-2. Blue Book. Issue 2. Washington, D.C.: CCSDS, July 2006.

NOTE – Normative references are contained in 1.4.